AJRCCM Articles in Press. Published on 22-August-2019 as 10.1164/rccm.201903-0596SO

Respiratory Drive in Critically Ill Patients: Pathophysiology and Clinical Implications

Katerina Vaporidi[1], Evangelia Akoumianaki[1], Irene Telias[2,3], Ewan C. Goligher[2,4,5], Laurent Brochard[2,3*+], Dimitris Georgopoulos[1*]

[1]Department of Intensive Care Medicine, University Hospital of Heraklion, Medical School University of Crete, Greece. [2]Interdepartmental Division of Critical Care Medicine, University of Toronto, Toronto, Canada. [3]Keenan Research Center and Li Ka Shing Knowledge Institute, St. Michael´s Hospital, Toronto, Canada. [4]Department of Medicine, University Health Network, Toronto, Canada. [5]Toronto General Hospital Research Institute, Toronto, Canada

*Equal contribution

[+] Deputy Editor, AJRCCM (participation complies with American Thoracic Society requirements for recusal from review and decisions for authored works).

Corresponding Author: D. Georgopoulos, Professor of Medicine,
Director of Intensive Care Medicine Department,
University Hospital of Heraklion, School of Medicine,
University of Crete, Heraklion, Crete, Greece
e-mail: georgopd@uoc.gr
Phone: +306944727501

Author's contributions: D.G. and L.B. contributed to the conception of this work. K.V., E.A., I.T. and D.G. drafted and reviewed the manuscript. All authors critically revised the manuscript for intellectually important content and gave final approval of the version to be submitted.

All sources of support: none

Running head: Respiratory drive in critically ill patients

Descriptor number: 4.08

Word count: 5572

This article has an online data supplement, which is accessible from this issue's table of contents online at www.atsjournals.org

AJRCCM Articles in Press. Published on 22-August-2019 as 10.1164/rccm.201903-0596SO

Abstract

The respiratory drive, the intensity of the respiratory centers output, determines the effort exerted in each breath. The increasing awareness of the adverse effects of both strong and weak respiratory efforts during mechanical ventilation on patient outcome brings our attention to the respiratory drive of the critically ill patient. Critical illness can affect patients' respiratory drive through multiple pathways, mainly operating through three feedback systems: a) cortical, b) metabolic and c) chemical. The chemical feedback system, defined as the response of the respiratory center's output to changes in arterial blood gases and pH, is one of the most important determinants of respiratory drive. The purpose of this state-of-the-art review is to describe the determinants of respiratory drive in critically ill patients, review the tools available to assess respiratory drive at the bedside, and discuss the implications of altered respiratory drive during mechanical ventilation. An analysis that relates the arterial carbon dioxide levels with brain's response to this stimulus will be presented, contrasting the brain's responses to the patient's ability to generate effective alveolar ventilation, both during unassisted breathing and with different modes of ventilatory assist. This analysis may facilitate comprehension of the pathophysiology of respiratory drive in critically ill patients. As we aim to avoid both over- and under-assistance with mechanical ventilation, considering the patients' respiratory drive at the bedside may improve clinical assessment and management of the patient and the ventilator.

Word count: 232

AJRCCM Articles in Press. Published on 22-August-2019 as 10.1164/rccm.201903-0596SO

Recent data indicate that during mechanical ventilation, both strong and weak respiratory efforts may adversely affect patient outcome through multiple pathways, such as patient-ventilator dyssynchrony, ventilation-induced lung injury (including patient-self-inflicted lung injury, P-SILI), diaphragmatic myotrauma, poor sleep quality, and cardiovascular compromise (1-6). It is important to recognize that the reason behind deleterious strong or weak respiratory efforts is a relatively high or low respiratory drive. In addition, the broad term "respiratory distress", often described in critically ill patients as a reason for manipulating ventilation and sedation, implies high respiratory drive. It is therefore important for intensivists to recognize the determinants of respiratory drive in critically ill patients and, ideally, to assess the patient's respiratory drive and effort when setting and managing mechanical assist. In this review we summarize the physiological control of respiratory drive and its determinants, and discuss the effects of critical illness and mechanical ventilation on respiratory drive. We then describe the methods available to evaluate respiratory drive at the bedside and discuss the clinical implications of altered respiratory drive in critically ill patients. We will focus on an analysis that relates CO_2 production and elimination with the brain´s response to this stimulus, contrasting this response to the patient´s ability to generate effective alveolar ventilation. This analysis aims to facilitate our understanding of how different variables modify respiratory drive in critically ill patients and to support clinical assessment and decision-making.

Respiratory Drive and the Inspiratory Flow-Generation Pathway

Breathing is centrally controlled by the respiratory centers, a complex network of interconnected neurons in the medulla and pons. The respiratory centers receive rather constant (tonic) inputs from various sources which, through a complicated process, are

translated into an output with an oscillatory pattern (7-10). This output can be functionally divided into rhythm- and pattern-generating signals and regulates the three phases of the respiratory cycle: the inspiratory, post-inspiratory, and expiratory (7-11). The system employs 'gating' to modulate the inputs, meaning that the same tonic input may have a different effect on the respiratory centers depending on the phase of the respiratory cycle (12). For example, a given input (i.e. $PaCO_2$) activates the respiratory center during inspiration but not during expiration (Gate function, Figure 1).

During the inspiratory phase, the respiratory centers' output to the inspiratory muscles (electrical activity, EA_{brain}) gradually rises, eventually reaching a peak value. Thereafter, the post-inspiratory phase begins and this output subsides to the baseline value. Finally, the expiratory phase commences, during which there is no respiratory center activity at resting breathing in healthy individuals. The duration of these three phases, although not always discrete, determines the timing of the breath and thus breathing frequency, whereas the intensity of the output is referred to as **respiratory drive** (7-10, 12-14). The distinction is important since respiratory drive may change without any changes in breath timing (i.e. frequency) and vice versa (15, 16).

The respiratory centers' output during the inspiratory phase travels through the **inspiratory flow-generation pathway** (Figure 1): from the brainstem and upper cervical spine neurons to the nucleus of respiratory motoneurons, leading to activation and contraction of the inspiratory muscles, finally resulting in the generation of inspiratory flow (7-9, 17-19).

In humans, since the intensity of the respiratory centers' output, cannot be directly measured, respiratory drive is quantified using the average rate of increase of various indices of motor output that, under certain circumstances, reflect the EA_{brain}. Indeed, in healthy humans the respiratory drive determines the average rate of increase of (a) the

AJRCCM Articles in Press. Published on 22-August-2019 as 10.1164/rccm.201903-0596SO

electrical activity of respiratory motoneurons (mainly the phrenic nerve in quiet breathing, dEA_{ph}/dt), (b) the electrical activity of the diaphragm (dEA_{di}/dt) and, during strenuous breathing of other inspiratory muscles, and c) the transdiaphragmatic pressure (dP_{di}/dt), or pressure developed by all inspiratory muscles (dP_{mus}/dt). Finally, the transdiaphragmatic pressure (P_{di}) or P_{mus} is translated into flow (V') and volume (V) according to the equation of motion (Figure 1) (19-21).

Determinants of Respiratory Drive

The main inputs to the respiratory centers affecting the respiratory drive are the cortical and chemical feedback and the metabolic rate (7, 19, 20, 22). Reflex responses, such as the Hering-Breuer reflex affect mainly the duration of the inspiratory and expiratory phase of the breath (19, 23, 24). Cortical inputs may override the automatic control of breathing (i.e. voluntary apnea) (25, 26). In critically ill patients, sensory and emotional stimuli such as pain and anxiety, can significantly affect the respiratory drive (27, 28). Cortical inputs also mediate the effect of the wakefulness drive to breathe, as discussed below. Normally, in the absence of voluntary activity, the cerebral cortex exerts an inhibitory effect on the respiratory centers and decreases their output (29). High respiratory drive is common in critically ill patients with brain injury involving the cerebral cortex and is associated with poor outcome (30, 31). Although metabolic rate plays a key role in modulating the respiratory drive during exercise, linking CO_2 production and elimination, its role in critically ill patients is unclear (32, 33). The main determinant of respiratory drive in many critically ill patients (and the most studied) is the chemical feedback, which is the response of the respiratory centers to changes in arterial blood gases and pH. Systemic inflammation and afferents from the lung and chest wall, through poorly described pathways, may also have a strong influence on the

respiratory centers and can increase respiratory drive for a given chemical stimulus (33, 34).

Chemical feedback

1. Chemical feedback to changes in $PaCO_2$/pH

Changes in $PaCO_2$ (and pH) are sensed by both peripheral and central chemoreceptors, the latter located at the retrotrapezoid nucleus on the ventrolateral surface of the medulla, and induce changes in the respiratory centers' output (7-9).

At steady-state, the arterial $PaCO_2$ is determined by the intersection of two curves, the metabolic hyperbola and the $PaCO_2$-ventilation response curve (Figure 2) (20). The metabolic hyperbola describes $PaCO_2$ as a function of minute ventilation (V'_E), i.e., the change in $PaCO_2$ obtained by a given change in minute ventilation, based on the alveolar gas equation:

$$PaCO_2 = \frac{k \cdot V'CO_2}{V'_E \cdot \left(1 - \frac{V_D}{V_T}\right)}$$

($V'CO_2$: rate of CO_2 production, V_D/V_T: ratio of dead space to tidal volume). The $PaCO_2$-ventilation response curve describes the V'_E as a function of $PaCO_2$ (that is the change in V'_E induced by a change in $PaCO_2$).

The normal response to *hypercapnia*, e.g., in case of increases in dead space, CO_2 production or inspired concentration of CO_2, consists of a linear increase in ventilation in response to a rise in $PaCO_2$ (9, 35-37). The change in minute ventilation per unit of increase in $PaCO_2$ (Figure 2), varies widely in normal individuals, having an average value of 2-3 l/min/mmHg, and a range of 0.6-8 l/min/mmHg (19, 20, 35, 37). The normal response to *hypocapnia*, e.g. in case of excessive ventilation, depends on the wakefulness/sleep or sedation state. In awake subjects, below the eupneic $PaCO_2$ level (the normal $PaCO_2$ at rest), the slope of the curve deviates from linear becoming almost

AJRCCM Articles in Press. Published on 22-August-2019 as 10.1164/rccm.201903-0596SO

horizontal at a minimum level of ventilation (Figure 2), which is maintained despite hypocapnia, a phenomenon known as wakefulness drive to breathe (22, 38). The wakefulness drive to breathe varies among healthy subjects, and is affected by PaO_2 and pH (19, 20, 37, 39). During sleep or sedation, the slope remains mostly linear, and, as a result, progressive hypocapnia leads to apnea (35, 39-41). The $PaCO_2$ level that causes apnea is referred to as 'apneic threshold'; this level varies among healthy individuals and is also affected by PaO_2 and pH (Figure 2).

It is important to emphasize that, normally, the changes in ventilation are primarily achieved through changes in respiratory drive and V_T, while breathing frequency changes little over a wide range of $PaCO_2$. Breathing frequency increases significantly when respiratory drive is increased several-fold above resting ventilation and, in the absence of wakefulness drive to breathe, decreases abruptly to zero when $PaCO_2$ reaches the apneic threshold (2, 36, 38, 42-45) (Figure 3). Nevertheless, in patients with severe V_T constraints due to respiratory muscle weakness, or abnormal mechanics, even small increases in $PaCO_2$ may elicit significant increases in breathing frequency (42, 46, 47). Finally, as increasing breathing frequency decreases the duration of inspiratory phase (42, 46, 47), respiratory drive increases (the same peak output is achieved at shorter time).

2. Chemical feedback to changes in PaO_2

The main chemoreceptors mediating the ventilatory response to hypoxemia are the carotid bodies, small clusters of oxygen-sensitive cells located at the carotid bifurcation (7, 48). Hypoxemia increases respiratory drive and thus minute ventilation (49, 50), an effect which is modified by the $PaCO_2$ and acid-base status. In healthy subjects the respiratory drive changes minimally with mild hypoxemia (PaO_2 60-70

mmHg) but at lower PaO_2 increases progressively with hypoxemia (48, 50). Although PaO_2 is a relatively weaker modulator of respiratory drive than $PaCO_2$, PaO_2 may significantly affect the respiratory drive through changes of the ventilatory responses to $PaCO_2$ (37, 50, 51).

Effects of critical illness on the determinants of respiratory drive

A. Dissociation between respiratory drive and actual ventilation

As discussed above, a change in respiratory drive normally translates into a change in ventilation through the inspiratory flow-generation pathway (Figure 1). The relationship between changes in respiratory drive and the resulting change in ventilation depends on the integrity of the inspiratory flow-generation pathway. In critically ill patients this pathway is often compromised (impaired neuromuscular function, abnormal respiratory system mechanics, Figure 1). Therefore, in critically ill patients a change in respiratory drive does not usually result in the expected change in ventilation.

To better understand the dissociation between respiratory drive and the resulting ventilation we will introduce the terms '**brain curve**' and '**ventilation curve**'. The term '**brain curve**' refers to the minute ventilation that would theoretically result in response to $PaCO_2$ changes if the inspiratory flow-generation pathway was intact (Figure 4A). In other words, the brain curve represents the ventilation desired by the brain at any $PaCO_2$ level. The term '**ventilation curve**' refers to the actual changes in minute ventilation in response to changes in $PaCO_2$, as modified by any impairment in the inspiratory flow-generation pathway (Figure 4B). Accordingly, if the inspiratory flow-generation pathway is intact, the brain curve is identical to the ventilation curve; there is no dissociation and at a given $PaCO_2$ the desired ventilation is equal to actual ventilation.

AJRCCM Articles in Press. Published on 22-August-2019 as 10.1164/rccm.201903-0596SO

When the inspiratory flow-generation pathway is impaired by critical illness, the brain and ventilation curves dissociate, and the resulting $PaCO_2$ at a given level of respiratory drive is higher than the brain desires. This increased $PaCO_2$ stimulates a further increase in respiratory drive according to the brain curve and the resulting increase in ventilation is determined by the ventilation curve. Steady state is reached (i.e. no further increases in $PaCO_2$ or minute ventilation) at the intersection of the actual ventilation curve (not the brain curve) and the metabolic hyperbola (Figure 4B) (52-55). It is considered that the difference between the actual ventilation (i.e. the ventilation curve) and the needs based on afferent signals (i.e., the brain curve) is a major contributor of dyspnea (56, 57).

The reader should appreciate that these mathematically described curves and their relationships are simplified representations of experimental data, aiming to facilitate understanding of the effects of critical illness and mechanical ventilation on respiratory drive, and cannot be directly applied to compute the ventilatory demands of a critically ill patient.

B. Effects of Critical illness on the Brain curve, the Ventilation curve, and the Metabolic Hyperbola

1. Brain curve

The slope and position of the brain curve are considerably modified by PaO_2 and pH (Figure 2 and Table 1); hypoxemia and metabolic acidosis shift the curve upward and left (i.e. increasing ventilatory response to CO_2), while hyperoxemia and metabolic alkalosis shift the curve downward and right (i.e. decreasing ventilatory response to CO_2) (35, 37, 51, 58-60). Moreover, stimulation of lung and chest wall receptors due to various pathologies of the respiratory system may shift the brain curve to the left and increase its

slope, while sedatives and opioids have the opposite effect (33-35, 61, 62). Although these ventilatory responses to CO_2 have not been evaluated specifically in critically ill patients, clinical data support these experimental observations (42, 46, 52, 63).

2. *Ventilation curve*

The ventilation curve is affected by any impairment in the inspiratory flow-generation pathway (Figure 1 and Table 1). As a result, in critically ill patients during unassisted breathing, the ventilation curve is shifted to the right (to higher $PaCO_2$) and its slope is decreased compared to the brain curve (Figure 4B). Because of this dissociation between the brain and ventilation curve, the ventilation curve and the metabolic hyperbola intersect at a higher $PaCO_2$ than the one desired by the brain (Figure 4B).

3. *Metabolic hyperbola*

Several conditions common in critically ill patients can affect both components of the metabolic hyperbola equation, CO_2 production and alveolar ventilation, and thus shift the metabolic hyperbola (Figure 5 and Table 1). Increased muscle activity, both voluntary (such as during exercise) and involuntary (such as during shivering, agitation, or tachypnea) can dramatically increase CO_2 production (64-67). The production of CO_2 can also be affected, similarly to healthy subjects, by the type and amount of nutrition administered (68, 69), body temperature (70), and sleep/wakefulness/sedation states (71, 72). Alveolar ventilation is determined by V_D/V_T and thus is affected by lung disease, hyperinflation, instrumental dead space, and breathing pattern (73-76). For example, a rapid shallow breathing pattern would increase V_D/V_T and shift the metabolic hyperbola upwards. On the other hand, unloading the inspiratory muscles by mechanical ventilation

AJRCCM Articles in Press. Published on 22-August-2019 as 10.1164/rccm.201903-0596SO

would decrease CO_2 production and increase V_T (thus decreasing V_D/V_T), shifting the metabolic hyperbola downwards.

C. Effects of Mechanical Ventilation

When mechanical ventilation is used to assist breathing, the ventilation curve is determined not only by the respiratory drive, respiratory rate, and the inspiratory flow-generation pathway, but also by the mode of support, settings, and patient-ventilator interactions (19, 20, 24, 45, 77). In contrast to unassisted breathing, where the ventilation curve is always shifted downward from the brain curve (Figure 4), the ventilation curve can be shifted to either side of the brain curve by mechanical ventilation. That is because during mechanical ventilation the total pressure applied to the respiratory system (P_{TOT}) in each breath is the sum of P_{mus} and pressure provided by the ventilator (Paw). According to the equation of motion, P_{TOT} is dissipated to overcome Rrs and Ers, determining the volume time profile as follows:

$$P_{TOT} = P_{mus} + Paw = V' * Rrs + \Delta V * Ers + P_{EE}$$

where P_{EE} is elastic recoil pressure at the end of expiration (zero at passive functional residual capacity), and ΔV and V' are volume above end-expiratory lung volume and flow. To what extent Paw and P_{mus} contribute to V_T (and thus to ventilation) depends on several factors related to the patient and the ventilator (19, 77, 78).

The mode and settings of assisted ventilatory support exert a tremendous influence on the ventilation curve and thus on the resulting $PaCO_2$ and respiratory drive (19, 77, 78). We will focus on three main modes of assisted mechanical ventilation: 1) assist volume control (AVC, V_T is constant), 2) pressure support (PS, pressure is constant) and 3) proportional assist modes (proportional assist ventilation with load adjustable gain factors, PAV+, and neurally adjusted ventilatory assist, NAVA, in which

neither pressure nor volume are constant but patient's effort drives airway pressure). These various modes modify the ventilation curve by adding the ventilator pressure (Paw) to Pmus (Figure 6).

To understand the effect of ventilator delivered pressure on the ventilation curve, we need first to describe the relationships between peak Pmus per breath ($Pmus_{peak}$) and the resulting V_T or V'_E under different modes of ventilation (Figures E1 and E2). These relationships are qualitatively similar to $PaCO_2$-V_T and $PaCO_2$-V'_E because $Pmus_{peak}$ increases linearly with increasing $PaCO_2$ (Figure 6).

1. Unassisted breathing

During unassisted breathing, at given (constant) respiratory system mechanics and end-expiratory lung volume, the $Pmus_{peak}$-V_T relationship is linear and its slope depends exclusively on respiratory system mechanics (Figure E1) (41, 46). Obviously, at a given respiratory rate the $Pmus_{peak}$-V'_E is also linear, but its slope depends both on respiratory system mechanics and respiratory rate.

2. Assist volume control (AVC) and Pressure support (PS)

With AVC the slope of the $Pmus_{peak}$-V_T relationship is always zero since the set V_T is essentially independent of patient's effort (horizontal line, constant V_T) (41, 46). This also entails that the ventilator-delivered pressure actually decreases with increasing $Pmus_{peak}$, in other words, the ventilator, in order to keep V_T at pre-set level, reduces assistance as patient respiratory effort increases. Of note, both the V_T and the peak-flow set by the clinician during AVC have an enormous impact on respiratory drive and thus on $Pmus_{peak}$ (79). During PS, a constant pressure is applied to respiratory system after triggering irrespective of $Pmus_{peak}$, resulting in a parallel up-ward shift of the unassisted breathing line without affecting its slope (Figure E1) (41, 46). With both AVC and PS, changing the level of assist (V_T or PS level) does not affect the slope but causes a parallel

AJRCCM Articles in Press. Published on 22-August-2019 as 10.1164/rccm.201903-0596SO

up-ward or down-ward shift of the curve (41, 46). It is important to note that V_T may be substantial even at very low $Pmus_{peak}$ (i.e. the patient relaxes all inspiratory muscles immediately after triggering), depending on the level of assist (41, 46). With AVC this V_T is pre-set, whereas with PS this V_T is referred to as minimum V_T and depends on the ventilator settings (the level of PS, rising time and the flow cycling threshold) and respiratory system mechanics (mainly Ers) (41, 46).

With both modes, at constant respiratory rate, the $Pmus_{peak}$-V_T relationship results in qualitatively similar $Pmus_{peak}$-V'_E and thus $PaCO_2$-V'_E relationships (Figures 6 and E2). If respiratory rate changes to a new constant value under AVC, the slope of the $Pmus_{peak}$-V'_E curve will remain zero and its position will be shifted, up-ward (with increasing respiratory rate) or down-ward (with decreasing respiratory rate), while under PS both the slope and position of the $Pmus_{peak}$-V'_E curve will be modified (Figures E2A and E2B). Under AVC at high respiratory drive, the slope of $Pmus_{peak}$-V'_E and $PaCO_2$-V'_E relationships may deviate from zero (increase), due to a progressive increase of patient respiratory rate, a common response pattern when V_T is constrained (42, 46, 47, 77) (Figure 6A, E4A). With PS, since respiratory rate changes little particularly when the respiratory drive is not very high (2), changes in drive often have a minimal influence on the slope of the ventilation curve.

3. Proportional assist modes

The effect of proportional assist modes on the $Pmus_{peak}$-V_T relation is fundamentally different: proportional ventilation effectively amplifies respiratory effort, increasing the slope of $Pmus_{peak}$-V_T relationship (41, 46). The magnitude of this increase depends on the level of assist (Figures 6 and E1). Unlike AVC and PS, under proportional assist modes relaxation of inspiratory muscles immediately after triggering

terminates the pressure delivered by the ventilator. In this case, even at very high assist, V_T will be zero or close to zero.

As with AVC and PS, with proportional modes (as with AVC and PS), at constant respiratory rate, the $Pmus_{peak}$-V_T relationship results in qualitatively similar $Pmus_{peak}$-V'_E and thus $PaCO_2$-V'_E relationships (Figures 6 and E2). However, with proportional modes, changes in respiratory rate modify the slope of $Pmus_{peak}$-V'_E curve but minimum ventilation is always close to zero (41, 80, 81) (Figure E2C). A more detailed description of the effects of varying levels of assist on respiratory drive with each mode is presented in the online supplement (Figures E3-6).

The actual $PaCO_2$ is determined by the intersection between the new ventilation curve (obtained by the patient's respiratory drive interacting with mechanical ventilatory support) and the metabolic hyperbola. In contrast to unassisted breathing, under mechanical ventilation this $PaCO_2$ may in fact be lower than the one the brain desires resulting in a decrease in respiratory drive. The respiratory drive is in either case determined by the ventilatory demands at the resulting $PaCO_2$ defined by the brain curve which, as discussed above, is modified by several other factors. Therefore, mechanical ventilation decreases respiratory drive indirectly by lowering $PaCO_2$ (24, 45, 82). However, in conscious patients, when unloading of inspiratory muscles by mechanical assist results in relief of distress, this may additionally decrease respiratory drive through cortical inputs (28).

Overall, critical illness is associated with variable changes in the metabolic hyperbola and a dissociation between the brain curve and the ventilation curve (Table 1). At steady-state, the $PaCO_2$ derives from the intersection of the metabolic hyperbola and the ventilation curve, both altered by critical illness and mechanical ventilation. The

AJRCCM Articles in Press. Published on 22-August-2019 as 10.1164/rccm.201903-0596SO

patient's respiratory drive is determined by the ventilation desired by the brain for this $PaCO_2$ (Figure 4B).

Measuring Respiratory Drive in Critically Ill Patients

As stated above, since the intensity of the respiratory centers' output cannot be directly measured, respiratory drive is quantified either by various indices of motor output or by the mean inspiratory flow (20, 83). The indices of motor output include the change in electrical activity of the diaphragm (EA_{di}), P_{di}, P_{mus} during inspiration, and the change in airway pressure observed during the inspiratory effort against occluded airways. When estimating the respiratory drive of critically ill patients it is important to recognize that the presence of a disease that affects the inspiratory flow-generation pathway at or prior to the anatomical site of measurement (closer to the respiratory center) always leads to under-estimation of the respiratory drive. Despite the limitations posed by critical illness, indices of respiratory drive may provide the physician information for the changes of respiratory drive over time, or in response to changes in ventilator settings. The methods available at the bedside to evaluate respiratory drive are described below, along with their limitations. In everyday practice, selecting which method to use in the individual patient depends, not only on the limitations of each method, but also on the availability of the equipment required for measurement acquisition and the complexity of the clinical condition.

A. Electrical activity of the diaphragm

Diaphragmatic electrical activity can be recorded using surface electrodes or via an esophageal catheter (81, 84, 85). It is, anatomically, the closest measurement to brain output that can be obtained at the bedside. The change in EA_{di} is linearly correlated with

the increase in ventilation stimulated by CO_2 rebreathing in healthy volunteers (86). In ARDS patients, EA_{di} increased with decreasing rates of extracorporeal CO_2 removal (87). Moreover, in mechanically ventilated patients, changes in P_{di} and $Pmus_{peak}$ were shown to follow changes in EA_{di} in response to changes in levels of pressure support and NAVA, respectively (88). It should be noted though that the EA_{di} signal does not have normal values. Thus, it can be used as a trend to monitor changes in the same patient (87-89). Finally, EA_{di} cannot evaluate the recruitment of accessory respiratory muscles (90).

B. Transdiaphragmatic and inspiratory pressure produced by all inspiratory muscles (P_{di} and P_{mus})

Diaphragmatic electrical activity is translated into P_{di}, which is measured using esophageal and gastric pressure sensors. As stated above, dP_{di}/dt quantifies respiratory drive if the pathway between the respiratory centers and the diaphragm pressure output is intact. Therefore, prerequisites include not only normal neural transmission but also normal muscle pressure generation for a given neural stimulation. During quiet breathing, dP_{di}/dt values of about 5 cmH_2O/sec are observed in healthy adults (91). As with all indices of respiratory drive, high dP_{di}/dt indicates high respiratory drive. On the other hand, normal or low dP_{di}/dt values do not necessarily entail normal or low drive unless intact neuromuscular function can be confirmed. Normalizing dP_{di}/dt for the maximum P_{di} takes into account abnormalities of inspiratory-flow generation pathway (19) but the latter can only be obtained in fully alert and cooperating patients.

In critically ill patients, diaphragmatic indices of respiratory drive may underestimate the true drive, particularly if it is high, due to the contribution of accessory inspiratory muscles to inspiratory pressure. Calculating the inspiratory pressure developed by all inspiratory muscles (P_{mus}) using the Campbell diagram may overcome

AJRCCM Articles in Press. Published on 22-August-2019 as 10.1164/rccm.201903-0596SO

this error (82, 92) but this method is cumbersome, relies on several assumptions, and is not suitable for every day clinical practice.

C. Airway occlusion pressure ($P_{0.1}$)

Airway occlusion pressure or $P_{0.1}$ is the drop in Paw at the first 100 msec of an inspiratory effort against an occluded airway. The rationale to use it as an indicator of drive is that $P_{0.1}$ increases proportionally to a rise in $PaCO_2$ (21, 93) and during the short occlusion: 1) Paw follows muscle pressure, 2) there is no significant behavioral or unconscious reaction, and 3) since no significant volume is displaced, abnormal respiratory mechanics do not affect the measurement. In healthy adults breathing at rest, $P_{0.1}$ ranges between 0.5 to 1.5 cmH_2O. In mechanically ventilated patients, values above 3.5 cmH_2O have been associated with elevated respiratory muscle effort (esophageal pressure-time product greater than 200 cm $H_2O \cdot$sec/min) and indicate high drive (94).

$P_{0.1}$ is easily obtained in the ICU as it is an automated measurement available on the majority of modern ventilators (95), but some issues need to be considered to properly interpret $P_{0.1}$ in critically ill patients. First, $P_{0.1}$ could underestimate respiratory drive in very severe muscle weakness because of impairment in the inspiratory flow-generation pathway. In moderate-severe weakness, however, $P_{0.1}$ still increases reliably with increasing $PaCO_2$, implying that the initial part of muscle contraction is relatively spared (54). Second, intrinsic positive end-expiratory pressure (PEEPi) can introduce a bias resulting from a phase lag between the change in Pmus and the change in Paw during an occlusion. Nevertheless, $P_{0.1}$ was shown to be a reasonable estimate of drive in intubated patients with PEEPi (96). Third, the decrease in Paw at the beginning of a breath can result from relaxation of the expiratory muscles and the accuracy of $P_{0.1}$ as a measure of drive in this condition is unknown (93). Fourth, the initial shape of the Pmus-

time curve may be influenced by increased resistance, exercise, or positive pressure ventilation, giving rise to some noise in the measurement (19, 97, 98). Fifth, breath-to-breath variability of $P_{0.1}$ is significant, and the clinical measurement of $P_{0.1}$ should be taken from an average of 3 to 4 measurements (99). Notwithstanding these pitfalls, $P_{0.1}$ may provide indications of changes in drive.

D. Clinical signs and breathing pattern

Clinical signs of dyspnea and respiratory distress, whenever present, are good indicators of high drive, as dyspnea is directly linked to high drive (100, 101). A rapid shallow breathing pattern, the use of accessory inspiratory muscles, activation of expiratory muscles, tachycardia, hypertension, and diaphoresis have been associated with high respiratory drive (76, 101). Obviously, in patients with severe neuromuscular disease or cervical spine injury clinical signs of dyspnea may be blunted, as patients may not be able to recruit expiratory muscles or accessory inspiratory muscles, even in the presence of high respiratory drive.

Importantly, although it is generally accepted that tachypnea is an indicator of high drive and bradypnea of low drive, respiratory rate is a highly insensitive sign of increasing respiratory drive (2, 102). Even under normal conditions, respiratory rate has a rather large variability in between and within subjects. Moreover, respiratory rate changes little with changes in respiratory drive or ventilator support, until drive increases by more than 3-4 fold of resting value (2, 36, 38, 42-45).

Clinical Implications

Although respiratory drive may not be easily measured in the critically ill patient, and thresholds defining injurious high or low drive have not been defined, the clinical

AJRCCM Articles in Press. Published on 22-August-2019 as 10.1164/rccm.201903-0596SO

conditions associated with alterations in brain and ventilation curves are easily recognized in everyday practice. Assessment of respiratory drive may help to direct management of the patient and the ventilator.

A. Low respiratory drive

A low respiratory drive implies that the respiratory centers demand a relatively low minute ventilation at the current $PaCO_2$. This occurs when the brain curve is shifted downward and to the right and/or when the intersection between the ventilation curve and metabolic hyperbola is at lower $PaCO_2$ than the $PaCO_2$ desired by the respiratory center. The most common conditions associated with a downward shift of the brain curve in critically ill patients are sedation and metabolic alkalosis (60-62). In the presence of these conditions the physician should expect that the patient's brain would be satisfied with a minute ventilation resulting in a higher than normal $PaCO_2$. It is important to recognise that a $PaCO_2$ that is lower than the $PaCO_2$ desired by the brain occurs only as a result of mechanical ventilation (i.e. overassistance), since all disease processes decrease ventilation output for a given respiratory center output.

Potential adverse consequences of low respiratory drive include weak inspiratory efforts resulting in disuse diaphragm atrophy (6, 103), patient-ventilator dyssynchronies (20, 104), and sleep disruption (20, 41). It is not uncommon that the decrease in respiratory drive is such that patients with conventional modes of support (volume or pressure) relax the diaphragm immediately after triggering (Figures E1, E2A and E2B). When the patient is sedated or asleep, and the delivered minute ventilation, as determined by the ventilator settings, results in a $PaCO_2$ level that reaches the apneic threshold, respiratory drive will hover around zero, and the patient will exhibit apneas and periodic breathing during assisted modes such as pressure support (Figures 6A-B, Figures E4D,

E5D) (105). Apneas cause sleep fragmentation, which has been associated with neurocognitive dysfunction, delirium, and autonomic nervous system dysfunction (105). The presence of apneas may affect ventilator management, as patients developing apneas are often placed for safety in controlled modes of ventilation thus unnecessarily prolonging weaning. Weak inspiratory efforts may result in diaphragmatic myotrauma, also prolonging weaning, and ICU stay (3, 4, 6, 89, 103, 106). Weak inspiratory efforts caused by low drive could also be falsely diagnosed as muscle weakness and mislead the clinical assessment.

B. High respiratory drive

A high respiratory drive implies that the respiratory centers demand a relatively high minute ventilation (1). This occurs when the intersection between ventilation curve and metabolic hyperbola is at $PaCO_2$ that is higher than the $PaCO_2$ desired by the brain (Figure 4). The deviation between actual and desired $PaCO_2$ will become larger if the brain curve is shifted left and/or has increased slope, a common scenario with metabolic acidosis and hypoxemia, but also with various pathologies that stimulate respiratory system receptors (lung and chest wall), or brain damage (30, 33, 34).

A high respiratory drive may be associated with rapid shallow breathing pattern and agitation (76, 101, 107) that increase both V_D/V_T and CO_2 production and move the metabolic hyperbola upwards, further increasing ventilatory demands and respiratory drive. Such breathing pattern may be the result of constrains to tidal volume increase, due to impaired respiratory muscle output or abnormal mechanics, as commonly observed in patients failing a weaning trial (20, 47, 76, 108). Moreover, when the excessive effort is perceived by the patient, high respiratory drive causes dyspnea and respiratory distress

AJRCCM Articles in Press. Published on 22-August-2019 as 10.1164/rccm.201903-0596SO

(57, 100). The inability to generate high inspiratory effort in patients with high respiratory drive may also contribute to respiratory distress and dyspnea (56, 109).

High respiratory drive leading to strong inspiratory efforts can promote patient-ventilator dysynchrony (20, 77), increase oxygen cost of breathing (67), while concomitantly increasing lung distending pressures, thus potentially placing patients at risk for patient self-inflicted lung injury (P-SILI) and inspiratory muscle damage (5, 110, 111). Although there is no direct evidence in humans that links strong inspiratory efforts to P-SILI and inspiratory muscle damage, experimental studies and indirect data in critically ill patients indicate that both matters should be of concern for the management of these patients (1, 111-114). Strong inspiratory efforts in pressure-regulated modes can result in the delivery of high tidal volume. In volume-regulated modes strong efforts can result in double triggering, increasing tidal volume, or increased regional stress in dependent areas, even without increase in tidal volume (114). Also, with proportional modes, high respiratory drive may override the protective mechanisms of control of breathing, particularly when Crs is low (<30 cmH_2O/l) (112) and lead to lung injury (102, 115).

The ability of critically ill patients to increase muscle pressure (P_{mus}) in response to increased respiratory drive is often limited. Healthy subjects can sustain indefinitely an increase in P_{mus} up to 50-60% of maximum inspiratory muscle pressure (P_{max}) in each breath although with further increases in load, contractile fatigue ensues and endurance time decreases progressively (116). Maintaining a very high fraction of P_{max} per breath may result, as a terminal event, in a decrease of respiratory drive to the point of central apnea/fatigue (117, 118). Endurance time is also affected by the duty cycle; it decreases with increasing T_I/T_{TOT} (119). Since in the majority of critically ill patients P_{max} is markedly reduced for a variety of reasons (19, 120), the level of respiratory drive that

AJRCCM Articles in Press. Published on 22-August-2019 as 10.1164/rccm.201903-0596SO

results in an unsustainable P_{mus} may be considerably decreased; a P_{mus} of 10 cmH_2O represents an insignificant load in a patient with near normal P_{max} (100 cmH_2O) but may be unsustainable in a patient with P_{max} of 20 cmH_2O. Thus, the patient with high respiratory drive and muscle weakness, unable to increase ventilation when needed, would develop dyspnea, respiratory distress, rapid shallow breathing, dysynchronies and gas exchange abnormalities (20, 107, 108, 121).

Conclusions

Critical illness affects the patient's respiratory drive through multiple mechanisms. The presence of high respiratory drive may induce injurious strenuous breathing and dyspnea, while low respiratory drive may lead to weak inspiratory efforts and apneas. Considering the determinants of patient's respiratory drive at the bedside may facilitate a better understanding and management of the patient and the ventilator, potentially avoiding some of the complications associated with high and low respiratory drive.

AJRCCM Articles in Press. Published on 22-August-2019 as 10.1164/rccm.201903-0596SO

References

1. Telias I, Brochard L, Goligher EC. Is my patient's respiratory drive (too) high? *Intensive Care Med* 2018; 44: 1936-1939.
2. Akoumianaki E, Vaporidi K, Georgopoulos D. The Injurious Effects of Elevated or Nonelevated Respiratory Rate during Mechanical Ventilation. *Am J Respir Crit Care Med* 2019; 199: 149-157.
3. Goligher EC, Fan E, Herridge MS, Murray A, Vorona S, Brace D, Rittayamai N, Lanys A, Tomlinson G, Singh JM, Bolz SS, Rubenfeld GD, Kavanagh BP, Brochard LJ, Ferguson ND. Evolution of Diaphragm Thickness during Mechanical Ventilation. Impact of Inspiratory Effort. *Am J Respir Crit Care Med* 2015; 192: 1080-1088.
4. Goligher EC, Dres M, Fan E, Rubenfeld GD, Scales DC, Herridge MS, Vorona S, Sklar MC, Rittayamai N, Lanys A, Murray A, Brace D, Urrea C, Reid WD, Tomlinson G, Slutsky AS, Kavanagh BP, Brochard LJ, Ferguson ND. Mechanical Ventilation-induced Diaphragm Atrophy Strongly Impacts Clinical Outcomes. *Am J Respir Crit Care Med* 2018; 197: 204-213.
5. Brochard L. Ventilation-induced lung injury exists in spontaneously breathing patients with acute respiratory failure: Yes. *Intensive Care Med* 2017; 43: 250-252.
6. Hudson MB, Smuder AJ, Nelson WB, Bruells CS, Levine S, Powers SK. Both high level pressure support ventilation and controlled mechanical ventilation induce diaphragm dysfunction and atrophy. *Crit Care Med* 2012; 40: 1254-1260.
7. Del Negro CA, Funk GD, Feldman JL. Breathing matters. *Nat Rev Neurosci* 2018; 19: 351-367.
8. Richter DW, Smith JC. Respiratory rhythm generation in vivo. *Physiology (Bethesda)* 2014; 29: 58-71.
9. Guyenet PG, Bayliss DA. Neural Control of Breathing and CO2 Homeostasis. *Neuron* 2015; 87: 946-961.
10. Ikeda K, Kawakami K, Onimaru H, Okada Y, Yokota S, Koshiya N, Oku Y, Iizuka M, Koizumi H. The respiratory control mechanisms in the brainstem and spinal cord: integrative views of the neuroanatomy and neurophysiology. *J Physiol Sci* 2017; 67: 45-62.
11. Agostoni E, Citterio G, D'Angelo E. Decay rate of inspiratory muscle pressure during expiration in man. *Respir Physiol* 1979; 36: 269-285.
12. Eldridge F.L. MDE. Oscillation, Gating, and Memory in the Respiratory Control System. Comprehensive Physiology; 2011. p. 93-114.

13. Mulkey DK, Stornetta RL, Weston MC, Simmons JR, Parker A, Bayliss DA, Guyenet PG. Respiratory control by ventral surface chemoreceptor neurons in rats. *Nat Neurosci* 2004; 7: 1360-1369.

14. Kam K, Worrell JW, Janczewski WA, Cui Y, Feldman JL. Distinct inspiratory rhythm and pattern generating mechanisms in the preBotzinger complex. *J Neurosci* 2013; 33: 9235-9245.

15. Corne S, Webster K, McGinn G, Walter S, Younes M. Medullary metastasis causing impairment of respiratory pressure output with intact respiratory rhythm. *Am J Respir Crit Care Med* 1999; 159: 315-320.

16. Costa R, Navalesi P, Cammarota G, Longhini F, Spinazzola G, Cipriani F, Ferrone G, Festa O, Antonelli M, Conti G. Remifentanil effects on respiratory drive and timing during pressure support ventilation and neurally adjusted ventilatory assist. *Respir Physiol Neurobiol* 2017; 244: 10-16.

17. Zaki Ghali MG, Britz G, Lee KZ. Pre-phrenic interneurons: Characterization and role in phrenic pattern formation and respiratory recovery following spinal cord injury. *Respir Physiol Neurobiol* 2018.

18. Wu J, Capelli P, Bouvier J, Goulding M, Arber S, Fortin G. A V0 core neuronal circuit for inspiration. *Nat Commun* 2017; 8: 544.

19. Younes M. GD. Control of breathing relevant to mechanical ventilation. New York: Marcel Dekker; 1998. p. 1-74.

20. Tobin MJ, Laghi F, Jubran A. Ventilatory failure, ventilator support, and ventilator weaning. *Compr Physiol* 2012; 2: 2871-2921.

21. Whitelaw WA, Derenne JP, Milic-Emili J. Occlusion pressure as a measure of respiratory center output in conscious man. *Respir Physiol* 1975; 23: 181-199.

22. Mahamed S, Ali AF, Ho D, Wang B, Duffin J. The contribution of chemoreflex drives to resting breathing in man. *Exp Physiol* 2001; 86: 109-116.

23. Hamilton RD, Winning AJ, Horner RL, Guz A. The effect of lung inflation on breathing in man during wakefulness and sleep. *Respir Physiol* 1988; 73: 145-154.

24. Kondili E, Prinianakis G, Anastasaki M, Georgopoulos D. Acute effects of ventilator settings on respiratory motor output in patients with acute lung injury. *Intensive Care Med* 2001; 27: 1147-1157.

25. Mador MJ, Tobin MJ. Effect of alterations in mental activity on the breathing pattern in healthy subjects. *Am Rev Respir Dis* 1991; 144: 481-487.

26. Raux M, Straus C, Redolfi S, Morelot-Panzini C, Couturier A, Hug F, Similowski T. Electroencephalographic evidence for pre-motor cortex activation during inspiratory loading in humans. *J Physiol* 2007; 578: 569-578.

AJRCCM Articles in Press. Published on 22-August-2019 as 10.1164/rccm.201903-0596SO

27. Tipton MJ, Harper A, Paton JFR, Costello JT. The human ventilatory response to stress: rate or depth? *J Physiol* 2017; 595: 5729-5752.

28. Raux M, Ray P, Prella M, Duguet A, Demoule A, Similowski T. Cerebral cortex activation during experimentally induced ventilator fighting in normal humans receiving noninvasive mechanical ventilation. *Anesthesiology* 2007; 107: 746-755.

29. Leitch AG, McLennan JE, Balkenhol S, McLaurin RL, Loudon RG. Ventilatory response to transient hyperoxia in head injury hyperventilation. *J Appl Physiol Respir Environ Exerc Physiol* 1980; 49: 52-58.

30. Esnault P, Roubin J, Cardinale M, D'Aranda E, Montcriol A, Cungi PJ, Goutorbe P, Joubert C, Dagain A, Meaudre E. Spontaneous Hyperventilation in Severe Traumatic Brain Injury: Incidence and Association with Poor Neurological Outcome. *Neurocrit Care* 2019; 30: 405-413.

31. Williamson CA, Sheehan KM, Tipirneni R, Roark CD, Pandey AS, Thompson BG, Rajajee V. The Association Between Spontaneous Hyperventilation, Delayed Cerebral Ischemia, and Poor Neurological Outcome in Patients with Subarachnoid Hemorrhage. *Neurocrit Care* 2015; 23: 330-338.

32. Haouzi P. Theories on the nature of the coupling between ventilation and gas exchange during exercise. *Respir Physiol Neurobiol* 2006; 151: 267-279.

33. Dempsey JA, Smith CA. Pathophysiology of human ventilatory control. *Eur Respir J* 2014; 44: 495-512.

34. Jacono FJ, Peng YJ, Nethery D, Faress JA, Lee Z, Kern JA, Prabhakar NR. Acute lung injury augments hypoxic ventilatory response in the absence of systemic hypoxemia. *J Appl Physiol (1985)* 2006; 101: 1795-1802.

35. Duffin J. The chemoreflex control of breathing and its measurement. *Can J Anaesth* 1990; 37: 933-942.

36. Duffin J, Mohan RM, Vasiliou P, Stephenson R, Mahamed S. A model of the chemoreflex control of breathing in humans: model parameters measurement. *Respir Physiol* 2000; 120: 13-26.

37. Rebuck AS, Slutsky AS. Measurement of ventilatory responses to hypercapnia and hypoxia. New York: Marcel Dekker; 1981. p. 745-772.

38. Patrick W, Webster K, Puddy A, Sanii R, Younes M. Respiratory response to CO2 in the hypocapnic range in awake humans. *J Appl Physiol (1985)* 1995; 79: 2058-2068.

39. Skatrud JB, Dempsey JA. Interaction of sleep state and chemical stimuli in sustaining rhythmic ventilation. *J Appl Physiol Respir Environ Exerc Physiol* 1983; 55: 813-822.

40. Datta AK, Shea SA, Horner RL, Guz A. The influence of induced hypocapnia and sleep on the endogenous respiratory rhythm in humans. *J Physiol* 1991; 440: 17-33.

41. Meza S, Mendez M, Ostrowski M, Younes M. Susceptibility to periodic breathing with assisted ventilation during sleep in normal subjects. *J Appl Physiol (1985)* 1998; 85: 1929-1940.

42. Ranieri VM, Giuliani R, Mascia L, Grasso S, Petruzzelli V, Puntillo N, Perchiazzi G, Fiore T, Brienza A. Patient-ventilator interaction during acute hypercapnia: pressure-support vs. proportional-assist ventilation. *J Appl Physiol (1985)* 1996; 81: 426-436.

43. Scheid P, Lofaso F, Isabey D, Harf A. Respiratory response to inhaled CO2 during positive inspiratory pressure in humans. *J Appl Physiol (1985)* 1994; 77: 876-882.

44. Georgopoulos D, Mitrouska I, Bshouty Z, Webster K, Patakas D, Younes M. Respiratory response to CO2 during pressure-support ventilation in conscious normal humans. *Am J Respir Crit Care Med* 1997; 156: 146-154.

45. Xirouhaki N, Kondili E, Mitrouska I, Siafakas N, Georgopoulos D. Response of respiratory motor output to varying pressure in mechanically ventilated patients. *Eur Respir J* 1999; 14: 508-516.

46. Mitrouska J, Xirouchaki N, Patakas D, Siafakas N, Georgopoulos D. Effects of chemical feedback on respiratory motor and ventilatory output during different modes of assisted mechanical ventilation. *Eur Respir J* 1999; 13: 873-882.

47. Tobin MJ, Laghi F, Brochard L. Role of the respiratory muscles in acute respiratory failure of COPD: lessons from weaning failure. *J Appl Physiol (1985)* 2009; 107: 962-970.

48. Lopez-Barneo J, Gonzalez-Rodriguez P, Gao L, Fernandez-Aguera MC, Pardal R, Ortega-Saenz P. Oxygen sensing by the carotid body: mechanisms and role in adaptation to hypoxia. *Am J Physiol Cell Physiol* 2016; 310: C629-642.

49. Easton PA, Slykerman LJ, Anthonisen NR. Ventilatory response to sustained hypoxia in normal adults. *J Appl Physiol (1985)* 1986; 61: 906-911.

50. Duffin J. Measuring the ventilatory response to hypoxia. *J Physiol* 2007; 584: 285-293.

51. Volta CA, Alvisi V, Bertacchini S, Marangoni E, Ragazzi R, Verri M, Alvisi R. Acute effects of hyperoxemia on dyspnoea and respiratory variables during pressure support ventilation. *Intensive Care Med* 2006; 32: 223-229.

52. Aubier M, Murciano D, Fournier M, Milic-Emili J, Pariente R, Derenne JP. Central respiratory drive in acute respiratory failure of patients with chronic obstructive pulmonary disease. *Am Rev Respir Dis* 1980; 122: 191-199.

53. Doorduin J, Nollet JL, Roesthuis LH, van Hees HW, Brochard LJ, Sinderby CA, van der Hoeven JG, Heunks LM. Partial Neuromuscular Blockade during Partial Ventilatory Support in Sedated Patients with High Tidal Volumes. *Am J Respir Crit Care Med* 2017; 195: 1033-1042.

54. Holle RH, Schoene RB, Pavlin EJ. Effect of respiratory muscle weakness on P0.1 induced by partial curarization. *J Appl Physiol Respir Environ Exerc Physiol* 1984; 57: 1150-1157.

AJRCCM Articles in Press. Published on 22-August-2019 as 10.1164/rccm.201903-0596SO

55. Borel CO, Teitelbaum JS, Hanley DF. Ventilatory drive and carbon dioxide response in ventilatory failure due to myasthenia gravis and Guillain-Barre syndrome. *Crit Care Med* 1993; 21: 1717-1726.

56. Moosavi SH, Topulos GP, Hafer A, Lansing RW, Adams L, Brown R, Banzett RB. Acute partial paralysis alters perceptions of air hunger, work and effort at constant P(CO(2)) and V(E). *Respir Physiol* 2000; 122: 45-60.

57. Mendonca CT, Schaeffer MR, Riley P, Jensen D. Physiological mechanisms of dyspnea during exercise with external thoracic restriction: role of increased neural respiratory drive. *J Appl Physiol (1985)* 2014; 116: 570-581.

58. Linton RA, Poole-Wilson PA, Davies RJ, Cameron IR. A comparison of the ventilatory response to carbon dioxide by steady-state and rebreathing methods during metabolic acidosis and alkalosis. *Clin Sci Mol Med* 1973; 45: 239-249.

59. Tojima H, Kunitomo F, Okita S, Yuguchi Y, Tatsumi K, Kimura H, Kuriyama T, Watanabe S, Honda Y. Difference in the effects of acetazolamide and ammonium chloride acidosis on ventilatory responses to CO2 and hypoxia in humans. *Jpn J Physiol* 1986; 36: 511-521.

60. Javaheri S, Shore NS, Rose B, Kazemi H. Compensatory hypoventilation in metabolic alkalosis. *Chest* 1982; 81: 296-301.

61. Harper MH, Hickey RF, Cromwell TH, Linwood S. The magnitude and duration of respiratory depression produced by fentanyl and fentanyl plus droperidol in man. *J Pharmacol Exp Ther* 1976; 199: 464-468.

62. Akada S, Fagerlund MJ, Lindahl SG, Sakamoto A, Prabhakar NR, Eriksson LI. Pronounced depression by propofol on carotid body response to CO2 and K+-induced carotid body activation. *Respir Physiol Neurobiol* 2008; 160: 284-288.

63. Pesenti A, Rossi N, Calori A, Foti G, Rossi GP. Effects of short-term oxygenation changes on acute lung injury patients undergoing pressure support ventilation. *Chest* 1993; 103: 1185-1189.

64. Hickmann CE, Roeseler J, Castanares-Zapatero D, Herrera EI, Mongodin A, Laterre PF. Energy expenditure in the critically ill performing early physical therapy. *Intensive Care Med* 2014; 40: 548-555.

65. Frank SM, Fleisher LA, Olson KF, Gorman RB, Higgins MS, Breslow MJ, Sitzmann JV, Beattie C. Multivariate determinants of early postoperative oxygen consumption in elderly patients. Effects of shivering, body temperature, and gender. *Anesthesiology* 1995; 83: 241-249.

66. Robertson CH, Jr., Foster GH, Johnson RL, Jr. The relationship of respiratory failure to the oxygen consumption of, lactate production by, and distribution of blood flow among

respiratory muscles during increasing inspiratory resistance. *J Clin Invest* 1977; 59: 31-42.

67. Viale JP, Annat GJ, Bouffard YM, Delafosse BX, Bertrand OM, Motin JP. Oxygen cost of breathing in postoperative patients. Pressure support ventilation vs continuous positive airway pressure. *Chest* 1988; 93: 506-509.
68. Tappy L, Schwarz JM, Schneiter P, Cayeux C, Revelly JP, Fagerquist CK, Jequier E, Chiolero R. Effects of isoenergetic glucose-based or lipid-based parenteral nutrition on glucose metabolism, de novo lipogenesis, and respiratory gas exchanges in critically ill patients. *Crit Care Med* 1998; 26: 860-867.
69. Herve P, Simonneau G, Girard P, Cerrina J, Mathieu M, Duroux P. Hypercapnic acidosis induced by nutrition in mechanically ventilated patients: glucose versus fat. *Crit Care Med* 1985; 13: 537-540.
70. Manthous CA, Hall JB, Olson D, Singh M, Chatila W, Pohlman A, Kushner R, Schmidt GA, Wood LD. Effect of cooling on oxygen consumption in febrile critically ill patients. *Am J Respir Crit Care Med* 1995; 151: 10-14.
71. White DP, Weil JV, Zwillich CW. Metabolic rate and breathing during sleep. *J Appl Physiol (1985)* 1985; 59: 384-391.
72. Pestana D, Garcia-de-Lorenzo A, Madero R. Metabolic pattern and lipid oxidation during abdominal surgery: midazolam versus propofol. *Anesth Analg* 1996; 83: 837-843.
73. Kallet RH, Zhuo H, Liu KD, Calfee CS, Matthay MA, National Heart L, Blood Institute ANI. The association between physiologic dead-space fraction and mortality in subjects with ARDS enrolled in a prospective multi-center clinical trial. *Respir Care* 2014; 59: 1611-1618.
74. Lucangelo U, Blanch L. Dead space. *Intensive Care Med* 2004; 30: 576-579.
75. Sinha P, Flower O, Soni N. Deadspace ventilation: a waste of breath! *Intensive Care Med* 2011; 37: 735-746.
76. Jubran A. Rapid Shallow Breathing: Causes and Consequences. Berlin, Heidelberg: Springer; 2003. p. 161-168.
77. Kondili E, Prinianakis G, Georgopoulos D. Patient-ventilator interaction. *Br J Anaesth* 2003; 91: 106-119.
78. Goligher EC, Ferguson ND, Brochard LJ. Clinical challenges in mechanical ventilation. *Lancet* 2016; 387: 1856-1866.
79. Cinnella G, Conti G, Lofaso F, Lorino H, Harf A, Lemaire F, Brochard L. Effects of assisted ventilation on the work of breathing: volume-controlled versus pressure-controlled ventilation. *Am J Respir Crit Care Med* 1996; 153: 1025-1033.
80. Younes M. Proportional assist ventilation, a new approach to ventilatory support. Theory. *Am Rev Respir Dis* 1992; 145: 114-120.

AJRCCM Articles in Press. Published on 22-August-2019 as 10.1164/rccm.201903-0596SO

81. Sinderby C, Navalesi P, Beck J, Skrobik Y, Comtois N, Friberg S, Gottfried SB, Lindstrom L. Neural control of mechanical ventilation in respiratory failure. *Nat Med* 1999; 5: 1433-1436.

82. Georgopoulos D, Mitrouska I, Webster K, Bshouty Z, Younes M. Effects of inspiratory muscle unloading on the response of respiratory motor output to CO2. *Am J Respir Crit Care Med* 1997; 155: 2000-2009.

83. Laghi F. Assessment of respiratory output in mechanically ventilated patients. *Respir Care Clin N Am* 2005; 11: 173-199.

84. Bellani G, Bronco A, Arrigoni Marocco S, Pozzi M, Sala V, Eronia N, Villa G, Foti G, Tagliabue G, Eger M, Pesenti A. Measurement of Diaphragmatic Electrical Activity by Surface Electromyography in Intubated Subjects and Its Relationship With Inspiratory Effort. *Respir Care* 2018; 63: 1341-1349.

85. Lin L, Guan L, Wu W, Chen R. Correlation of surface respiratory electromyography with esophageal diaphragm electromyography. *Respir Physiol Neurobiol* 2019; 259: 45-52.

86. Luo YM, Hart N, Mustfa N, Lyall RA, Polkey MI, Moxham J. Effect of diaphragm fatigue on neural respiratory drive. *J Appl Physiol (1985)* 2001; 90: 1691-1699.

87. Mauri T, Grasselli G, Suriano G, Eronia N, Spadaro S, Turrini C, Patroniti N, Bellani G, Pesenti A. Control of Respiratory Drive and Effort in Extracorporeal Membrane Oxygenation Patients Recovering from Severe Acute Respiratory Distress Syndrome. *Anesthesiology* 2016; 125: 159-167.

88. Beck J, Gottfried SB, Navalesi P, Skrobik Y, Comtois N, Rossini M, Sinderby C. Electrical activity of the diaphragm during pressure support ventilation in acute respiratory failure. *Am J Respir Crit Care Med* 2001; 164: 419-424.

89. Carteaux G, Cordoba-Izquierdo A, Lyazidi A, Heunks L, Thille AW, Brochard L. Comparison Between Neurally Adjusted Ventilatory Assist and Pressure Support Ventilation Levels in Terms of Respiratory Effort. *Crit Care Med* 2016; 44: 503-511.

90. Poulsen MK, Thomsen LP, Mifsud NL, Nielsen NP, Jorgensen RM, Kjaergaard S, Karbing DS. Electrical activity of the diaphragm during progressive cycling exercise in endurance-trained men. *Respir Physiol Neurobiol* 2015; 205: 77-83.

91. Corne S, Webster K, Younes M. Effects of inspiratory flow on diaphragmatic motor output in normal subjects. *J Appl Physiol (1985)* 2000; 89: 481-492.

92. American Thoracic Society/European Respiratory S. ATS/ERS Statement on respiratory muscle testing. *Am J Respir Crit Care Med* 2002; 166: 518-624.

93. Whitelaw WA, Derenne JP. Airway occlusion pressure. *J Appl Physiol (1985)* 1993; 74: 1475-1483.

94. Rittayamai N, Beloncle F, Goligher EC, Chen L, Mancebo J, Richard JM, Brochard L. Effect of inspiratory synchronization during pressure-controlled ventilation on lung distension and inspiratory effort. *Ann Intensive Care* 2017; 7: 100.

95. Telias I, Damiani F, Brochard L. The airway occlusion pressure (P0.1) to monitor respiratory drive during mechanical ventilation: increasing awareness of a not-so-new problem. *Intensive Care Med* 2018; 44: 1532-1535.

96. Conti G, Cinnella G, Barboni E, Lemaire F, Harf A, Brochard L. Estimation of occlusion pressure during assisted ventilation in patients with intrinsic PEEP. *Am J Respir Crit Care Med* 1996; 154: 907-912.

97. Gallagher CG, Younes M. Effect of pressure assist on ventilation and respiratory mechanics in heavy exercise. *J Appl Physiol (1985)* 1989; 66: 1824-1837.

98. Derenne JP, Whitelaw WA, Couture J, Milic-Emili J. Load compensation during positive pressure breathing in anesthetized man. *Respir Physiol* 1986; 65: 303-314.

99. Kera T, Aihara A, Inomata T. Reliability of airway occlusion pressure as an index of respiratory motor output. *Respir Care* 2013; 58: 845-849.

100. Faisal A, Alghamdi BJ, Ciavaglia CE, Elbehairy AF, Webb KA, Ora J, Neder JA, O'Donnell DE. Common Mechanisms of Dyspnea in Chronic Interstitial and Obstructive Lung Disorders. *Am J Respir Crit Care Med* 2016; 193: 299-309.

101. Parshall MB, Schwartzstein RM, Adams L, Banzett RB, Manning HL, Bourbeau J, Calverley PM, Gift AG, Harver A, Lareau SC, Mahler DA, Meek PM, O'Donnell DE, American Thoracic Society Committee on D. An official American Thoracic Society statement: update on the mechanisms, assessment, and management of dyspnea. *Am J Respir Crit Care Med* 2012; 185: 435-452.

102. Mauri T, Langer T, Zanella A, Grasselli G, Pesenti A. Extremely high transpulmonary pressure in a spontaneously breathing patient with early severe ARDS on ECMO. *Intensive Care Med* 2016; 42: 2101-2103.

103. Zambon M, Beccaria P, Matsuno J, Gemma M, Frati E, Colombo S, Cabrini L, Landoni G, Zangrillo A. Mechanical Ventilation and Diaphragmatic Atrophy in Critically Ill Patients: An Ultrasound Study. *Crit Care Med* 2016; 44: 1347-1352.

104. Vitacca M, Bianchi L, Zanotti E, Vianello A, Barbano L, Porta R, Clini E. Assessment of physiologic variables and subjective comfort under different levels of pressure support ventilation. *Chest* 2004; 126: 851-859.

105. Weinhouse GL, Schwab RJ, Watson PL, Patil N, Vaccaro B, Pandharipande P, Ely EW. Bench-to-bedside review: delirium in ICU patients - importance of sleep deprivation. *Crit Care* 2009; 13: 234.

AJRCCM Articles in Press. Published on 22-August-2019 as 10.1164/rccm.201903-0596SO

106. Kim WY, Suh HJ, Hong SB, Koh Y, Lim CM. Diaphragm dysfunction assessed by ultrasonography: influence on weaning from mechanical ventilation. *Crit Care Med* 2011; 39: 2627-2630.

107. Jubran A, Tobin MJ. Pathophysiologic basis of acute respiratory distress in patients who fail a trial of weaning from mechanical ventilation. *Am J Respir Crit Care Med* 1997; 155: 906-915.

108. Tobin MJ, Perez W, Guenther SM, Semmes BJ, Mador MJ, Allen SJ, Lodato RF, Dantzker DR. The pattern of breathing during successful and unsuccessful trials of weaning from mechanical ventilation. *Am Rev Respir Dis* 1986; 134: 1111-1118.

109. Banzett RB, Lansing RW, Brown R, Topulos GP, Yager D, Steele SM, Londono B, Loring SH, Reid MB, Adams L, et al. 'Air hunger' from increased PCO2 persists after complete neuromuscular block in humans. *Respir Physiol* 1990; 81: 1-17.

110. Yoshida T, Uchiyama A, Matsuura N, Mashimo T, Fujino Y. Spontaneous breathing during lung-protective ventilation in an experimental acute lung injury model: high transpulmonary pressure associated with strong spontaneous breathing effort may worsen lung injury. *Crit Care Med* 2012; 40: 1578-1585.

111. Yoshida T, Uchiyama A, Matsuura N, Mashimo T, Fujino Y. The comparison of spontaneous breathing and muscle paralysis in two different severities of experimental lung injury. *Crit Care Med* 2013; 41: 536-545.

112. Vaporidi K, Psarologakis C, Proklou A, Pediaditis E, Akoumianaki E, Koutsiana E, Chytas A, Chouvarda I, Kondili E, Georgopoulos D. Driving pressure during proportional assist ventilation: an observational study. *Ann Intensive Care* 2019; 9: 1.

113. Papazian L, Forel JM, Gacouin A, Penot-Ragon C, Perrin G, Loundou A, Jaber S, Arnal JM, Perez D, Seghboyan JM, Constantin JM, Courant P, Lefrant JY, Guerin C, Prat G, Morange S, Roch A, Investigators AS. Neuromuscular blockers in early acute respiratory distress syndrome. *N Engl J Med* 2010; 363: 1107-1116.

114. Yoshida T, Nakahashi S, Nakamura MAM, Koyama Y, Roldan R, Torsani V, De Santis RR, Gomes S, Uchiyama A, Amato MBP, Kavanagh BP, Fujino Y. Volume-controlled Ventilation Does Not Prevent Injurious Inflation during Spontaneous Effort. *Am J Respir Crit Care Med* 2017; 196: 590-601.

115. Mascheroni D, Kolobow T, Fumagalli R, Moretti MP, Chen V, Buckhold D. Acute respiratory failure following pharmacologically induced hyperventilation: an experimental animal study. *Intensive Care Med* 1988; 15: 8-14.

116. Roussos CS, Macklem PT. Diaphragmatic fatigue in man. *J Appl Physiol Respir Environ Exerc Physiol* 1977; 43: 189-197.

117. Aleksandrova NP, Isaev GG. Central and peripheral components of diaphragmatic fatigue during inspiratory resistive load in cats. *Acta Physiol Scand* 1997; 161: 355-360.

118. Ferguson GT. Respiratory failure due to altered central drive during inspiratory loading in rabbits. *Respir Physiol* 1995; 99: 75-87.

119. Bellemare F, Grassino A. Effect of pressure and timing of contraction on human diaphragm fatigue. *J Appl Physiol Respir Environ Exerc Physiol* 1982; 53: 1190-1195.

120. Vassilakopoulos T, Zakynthinos S, Roussos C. Respiratory muscles and weaning failure. *Eur Respir J* 1996; 9: 2383-2400.

121. Laghi F, Cattapan SE, Jubran A, Parthasarathy S, Warshawsky P, Choi YS, Tobin MJ. Is weaning failure caused by low-frequency fatigue of the diaphragm? *Am J Respir Crit Care Med* 2003; 167: 120-127.

AJRCCM Articles in Press. Published on 22-August-2019 as 10.1164/rccm.201903-0596SO

Figure Legends

Figure 1: The Inspiratory flow-generation pathway. Gate: the effects of afferent signals (inputs) vary depending on the phase of the inspiratory cycle they arrive; C3-C5: cervical spine levels; EA_{ph}, dEA_{ph}/dt, $EA_{di,}$ dEA_{di}/dt: electrical activity and change over time of the phrenic nerve, and diaphragm during inspiratory phase, respectively; Pdi, dP_{di}/dt: trasdiaphragmatic pressure and change over time during the inspiratory phase; V': flow, ΔV: volume above end-expiratory lung volume, Rrs, Ers: respiratory system resistance and elastance, respectively; P_{EE}: elastic recoil pressure at end-expiration (zero at functional residual capacity). dV/dt: change in volume over time; V_T/T_I: tidal volume to inspiratory time ratio or mean inspiratory flow.

Figure 2: Relationship between $PaCO_2$ and minute ventilation obtained by the 1) graphical representation of the equation: $PaCO_2=0.863*V'CO_2/[V'_E*(1-V_D/V_T)]$, the metabolic hyperbola (gray line), and 2) The $PaCO_2$-ventilation response curve (the change in minute ventilation induced by a change in $PaCO_2$), during wakefulness (black solid line) and sleep (black dashed line) in a healthy subject. The intersection between the metabolic hyperbola and the ventilation curve defines $PaCO_2$ at steady state during wakefulness and sleep (open and closed circles, respectively). Voluntary hyper- or hypo-ventilation could change $PaCO_2$ anywhere along the metabolic hyperbola (white squares). V'_E: minute ventilation (l/min), $V'CO_2$: CO_2 production (ml/min), V_D/V_T: dead space to tidal volume ratio.

Figure 3: Changes in minute ventilation (upper panel), tidal volume (middle panel) and breathing frequency (lower panel) versus end-tidal PCO_2, obtained from healthy young volunteers by a CO_2-rebreathing test. Notice the two different slopes of ventilation increase (S1 and S2) and the corresponding change in slope in tidal volume and respiratory rate increase (T1 and T2 mark the breakpoints separating the three segments

of different slope). In this subject, and in 75% of the examined cases, breathing frequency increased significantly when minute ventilation (ventilatory demands) was several-fold higher than basal ventilation. On the contrary tidal volume (and thus effort per breath, proportional to respiratory drive) increased significantly when PCO_2 exceeded normal. From ref. 36 with permission.

Figure 4: A: Graphical representation of the metabolic hyperbola and brain/ventilation curve of a healthy human. The intersection of the metabolic hyperbola and ventilation curve (open circle) determines the steady-state $PaCO_2$ and minute ventilation (V'_E), 40 mmHg and 6.2 L/min, respectively (please note that these mathematically described curves and relationships are simplified presentations of experimental data, aiming to facilitate understanding of the effects of critical illness and mechanical ventilation on respiratory drive, and cannot be directly applied to compute the ventilatory demands of a critically ill patient).

B: This human develops severe pneumonia, causing increased CO_2 production ($V'CO_2$) and dead space to tidal volume ratio (V_D/V_T) which move the metabolic hyperbola upward, and hypoxemia, which moves the brain curve to the left and increases its slope. Due to increased Ers, a given respiratory centers output per minute (RCO/min) results in a lower V'_E, thus the slope of the ventilation curve is shifted downwards. A dissociation of the ventilation curve from the brain curve occurs. In the presence of a dissociation, any change in $PaCO_2$ alters the RCO/min (mainly due to change in respiratory drive, RCO per breath), as much as the brain curve dictates, and any change in RCO/min can only change the actual ventilation as much as the ventilation curve dictates. Assuming for simplicity that the change in Ers, and thus the deviation of ventilation curve, occurs abruptly, the RCO/min corresponds initially to point 1 (V'_E 17.5 l/min), whereas the actual V'_E drops to point 2 (4.5 l/min). This decrease in ventilation leads to a gradual

AJRCCM Articles in Press. Published on 22-August-2019 as 10.1164/rccm.201903-0596SO

increase of $PaCO_2$, which in turn stimulates the respiratory center. The RCO/min progressively increases along the brain curve (from point 1 to 3), following the increase in $PaCO_2$. In parallel, this increase in RCO/min results in an increase in the actual V'_E along the ventilation curve (from point 2 to 4). When RCO/min (point 3) results in an actual V'_E at intersection of the ventilation curve and metabolic hyperbola (point 4) a steady state occurs, $PaCO_2$ stabilizes, and respiratory drive, RCO/min and V'_E do not increase further. Although brain's ventilation demands (46 L/min) are not met (actual V'_E=13 L/min) respiratory drive and RCO/min do not increase further, since the CO_2 stimulus is constant.

Figure 5: Metabolic hyperbola shifts from changes in dead space to tidal volume ratio (V_D/V_T) and CO_2 production ($V'CO_2$). Vertical dotted lines indicate the different $PaCO_2$ which would result if ventilation was the same (10 L/min) in all cases. Horizontal dotted lines indicate the different minute ventilation required to maintain the same PCO_2 (40 mmHg) in all cases.

Figure 6: Effects of different modes of assisted mechanical ventilation on the ventilation curve and respiratory drive in a sedated patient in whom the un-assisted ventilation curve (black solid line) deviates from brain curve (black dashed line). For simplicity, metabolic hyperbola (gray line) and respiratory rate are constant in all conditions. Apneic threshold is set at $PaCO_2$ of 35 mmHg. In each mode two levels of assist are shown (low and high, red lines). With all modes at low levels of assist, steady state occurs (open circles) while $PaCO_2$ is lower than the $PaCO_2$ during un-assisted breathing (intersection between un-assisted ventilation curve and metabolic hyperbola), but higher than the $PaCO_2$ desired by the brain (intersection between brain curve and metabolic hyperbola). The respiratory center output (RCO)/min is determined by the brain curve, at this $PaCO_2$ (dark circle). At high level of assist the intersection between ventilation curve and metabolic hyperbola is

AJRCCM Articles in Press. Published on 22-August-2019 as 10.1164/rccm.201903-0596SO

at lower $PaCO_2$ than that desired by the brain. With assist-volume (A) and pressure support (B) a non-steady state occurs in this example, since the intersection of the metabolic hyperbola and the ventilation curve (open squares) is at a $PaCO_2$ lower than the apneic threshold, respiratory drive hovers around zero, and the occurrence of apneas maintains $PaCO_2$ close to apneic threshold (black squares). With proportional modes (C) even at highest assist (slope almost 90^o) a steady state is achieved (open circle) and RCO/min and respiratory drive although low, are always above zero (dark circle).

AJRCCM Articles in Press. Published on 22-August-2019 as 10.1164/rccm.201903-0596SO

Table 1: Conditions affecting the position of the brain and ventilation curve, and the metabolic hyperbola

Brain curve	**Upwards/Left shift**	**Downwards/right shift**
	Metabolic acidosis	Metabolic alkalosis
	Hypoxemia	Hyperoxemia
	Interstitial lung edema	Sedation
	Brain pathology (cortical)	Brain pathology (brain stem)
Ventilation curve	**Upwards/Left shift**	**Downwards/right shift**
	Mechanical ventilation	Upper motor neuron disease
	Partial or full recovery from diseases that affects Inspiratory-flow generation pathway (upward shift from disease state, towards normal)	Diseases affecting nerve conduction (Guillain-Barre)
		Diseases affecting neuromuscular junction (myasthenia Gravis)
		Respiratory muscle weakness/injury
		Impaired diaphragm length-tension relationship
		Increased airway resistance
		Decreased respiratory system compliance
Metabolic Hyperbola	**Upwards shift Increased V_D/V_T, Increased $V'CO_2$**	**Downwards shift Decreased V_D/V_T or Decreased $V'CO_2$**
	Low tidal volume (V_D/V_T)	High tidal volume (V_D/V_T)
	Rapid shallow breathing (V_D/V_T)	Sedation ($V'CO_2$)
	Increased dead space - lung pathology (V_D/V_T)	Hypothermia ($V'CO_2$)
	Increased dead space – ventilator circuit (V_D/V_T)	
	Agitation/ shivering ($V'CO_2$)	
	Fever ($V'CO_2$)	
	Strenuous breathing ($V'CO_2$)	

V_D/V_T: dead space to tidal volume ratio, $V'CO_2$: CO_2 production.

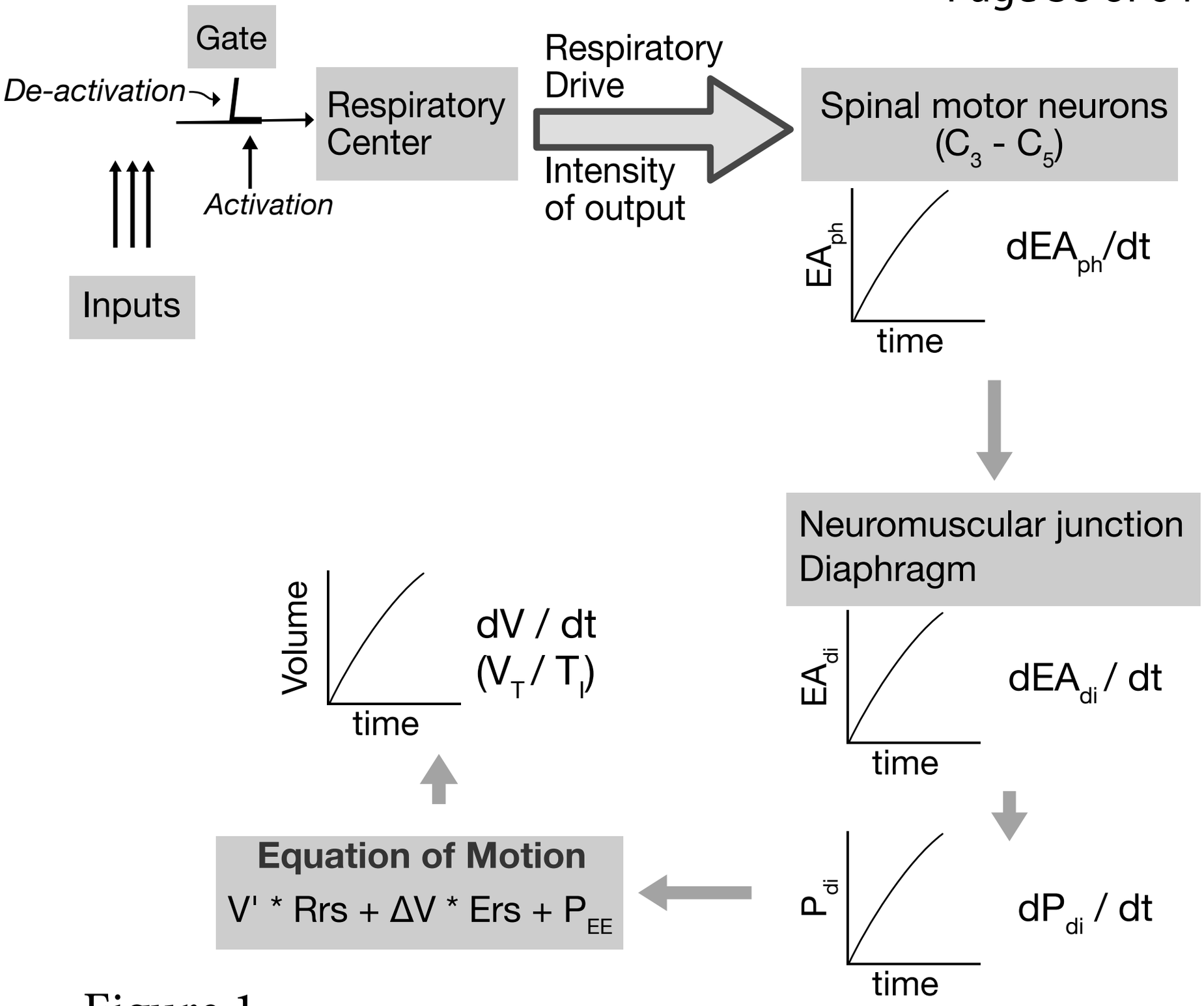

Figure 1

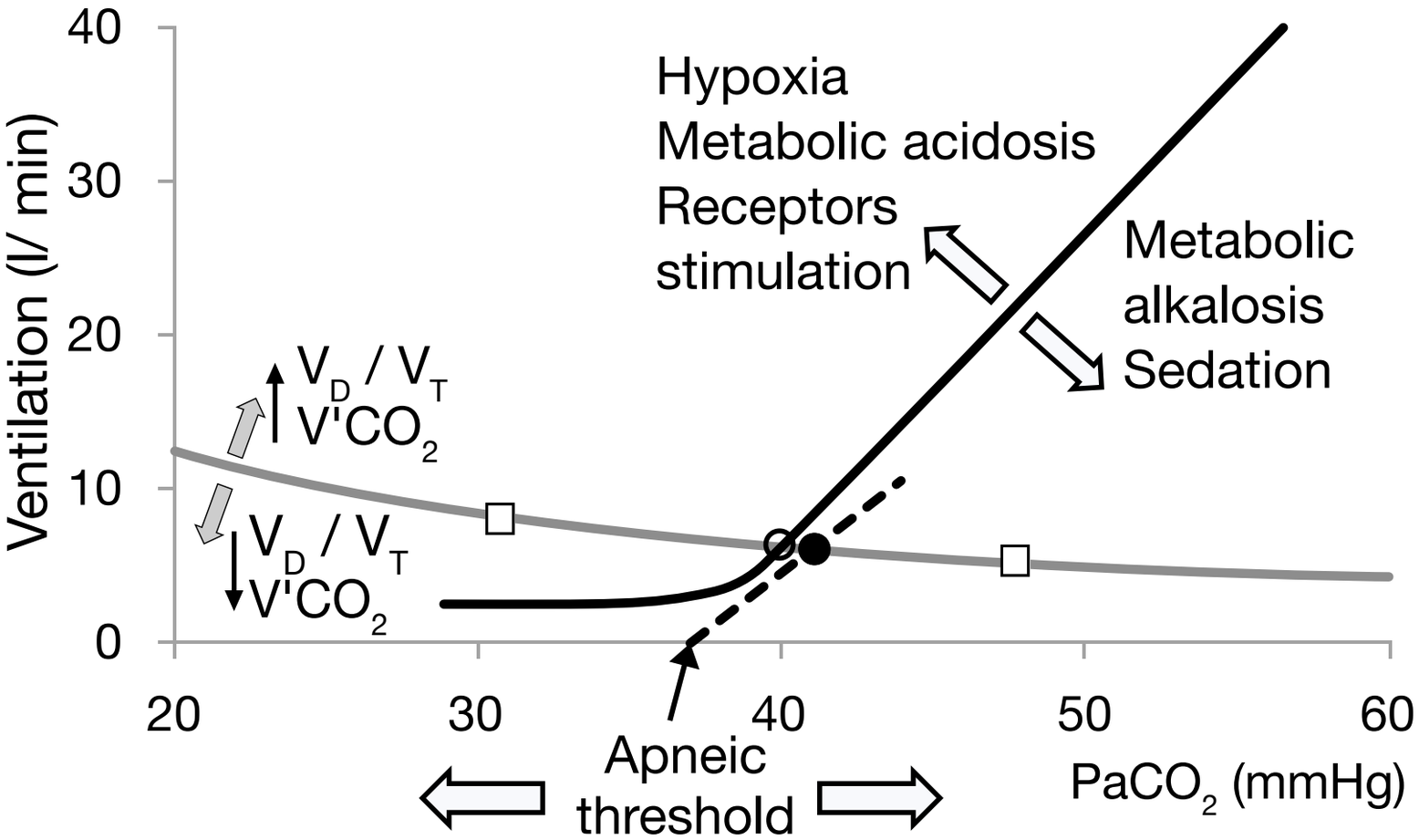

Figure 2

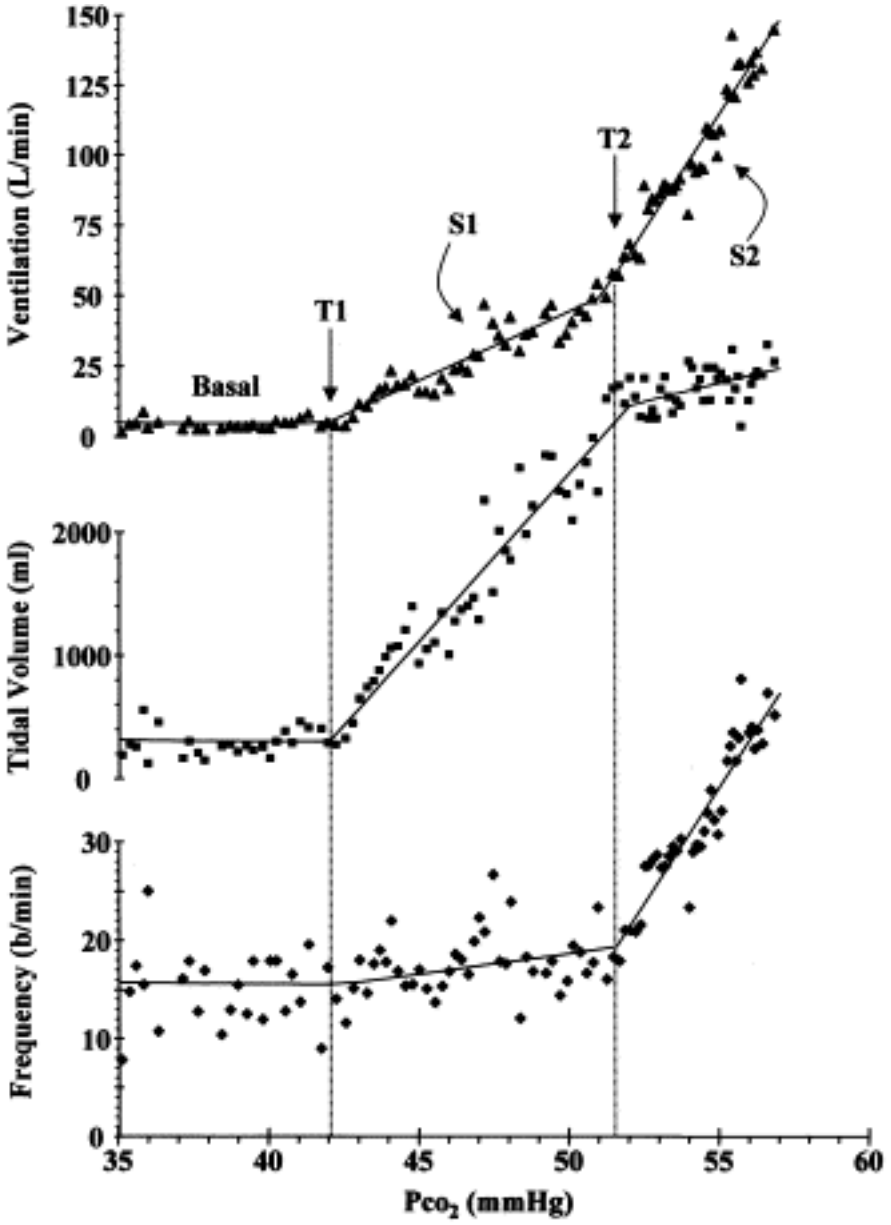

Figure 3

AJRCCM Articles in Press. Published on 22-August-2019 as 10.1164/rccm.201903-0596SO

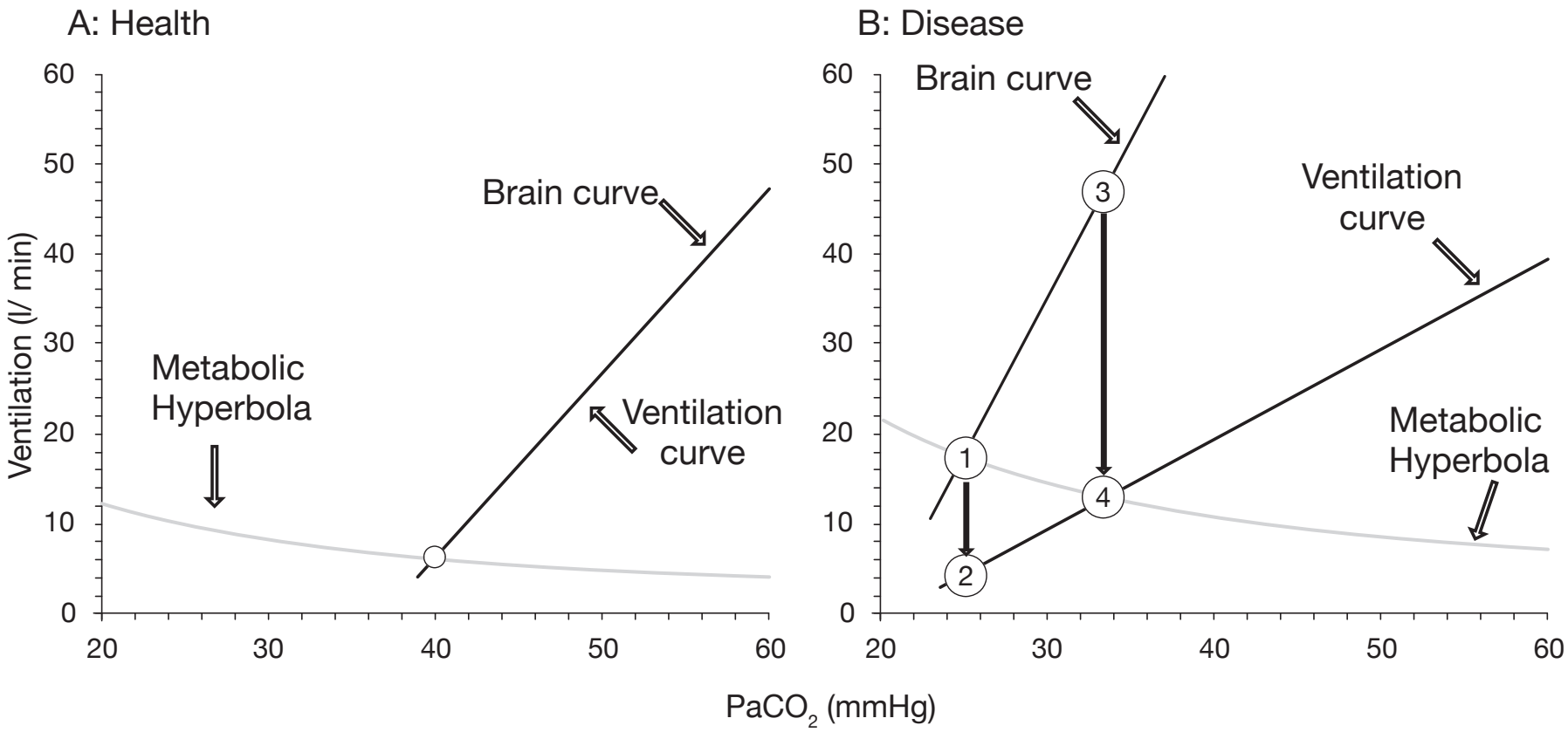

Figure 4

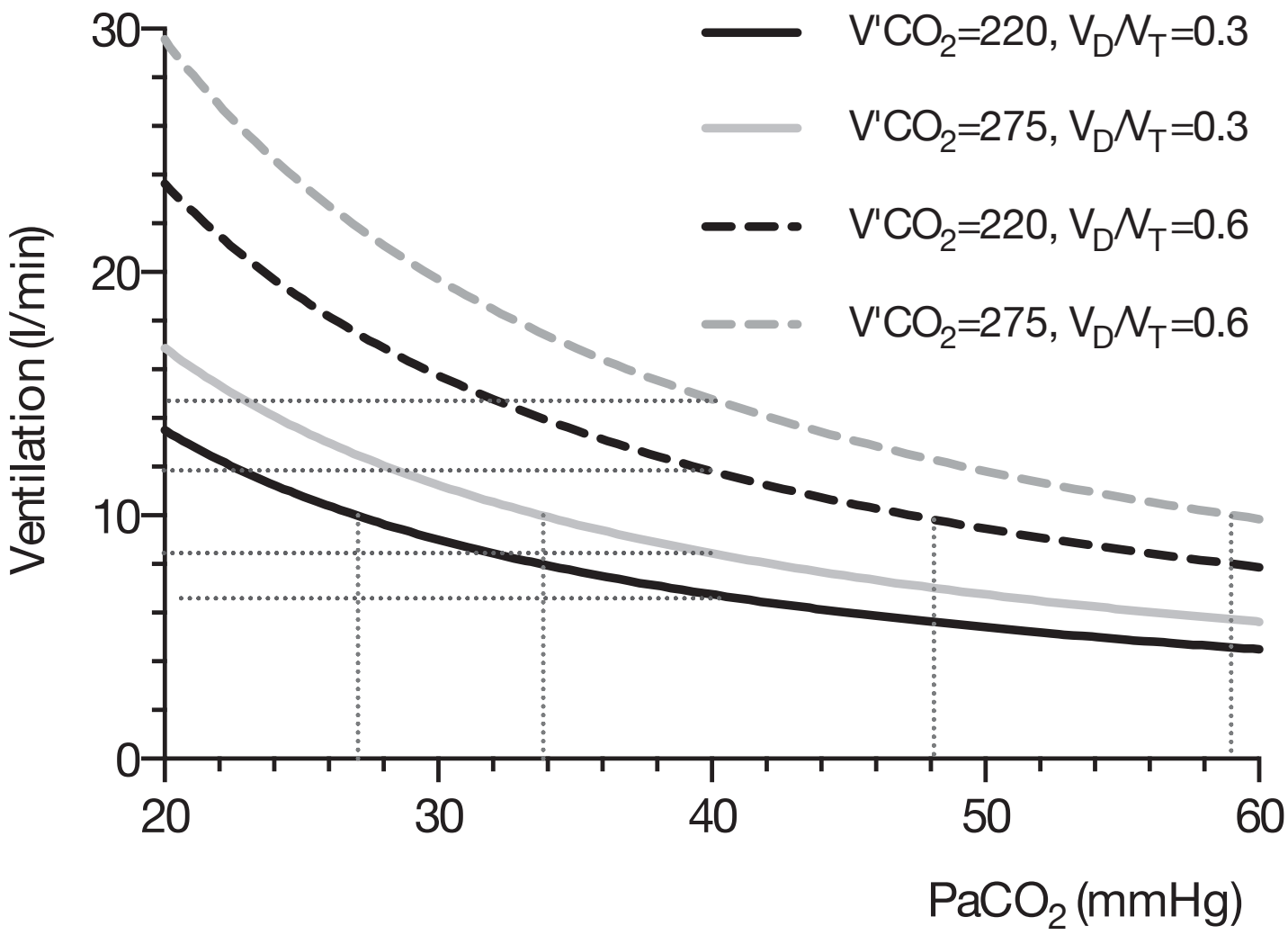

Figure 5

AJRCCM Articles in Press. Published on 22-August-2019 as 10.1164/rccm.201903-0596SO

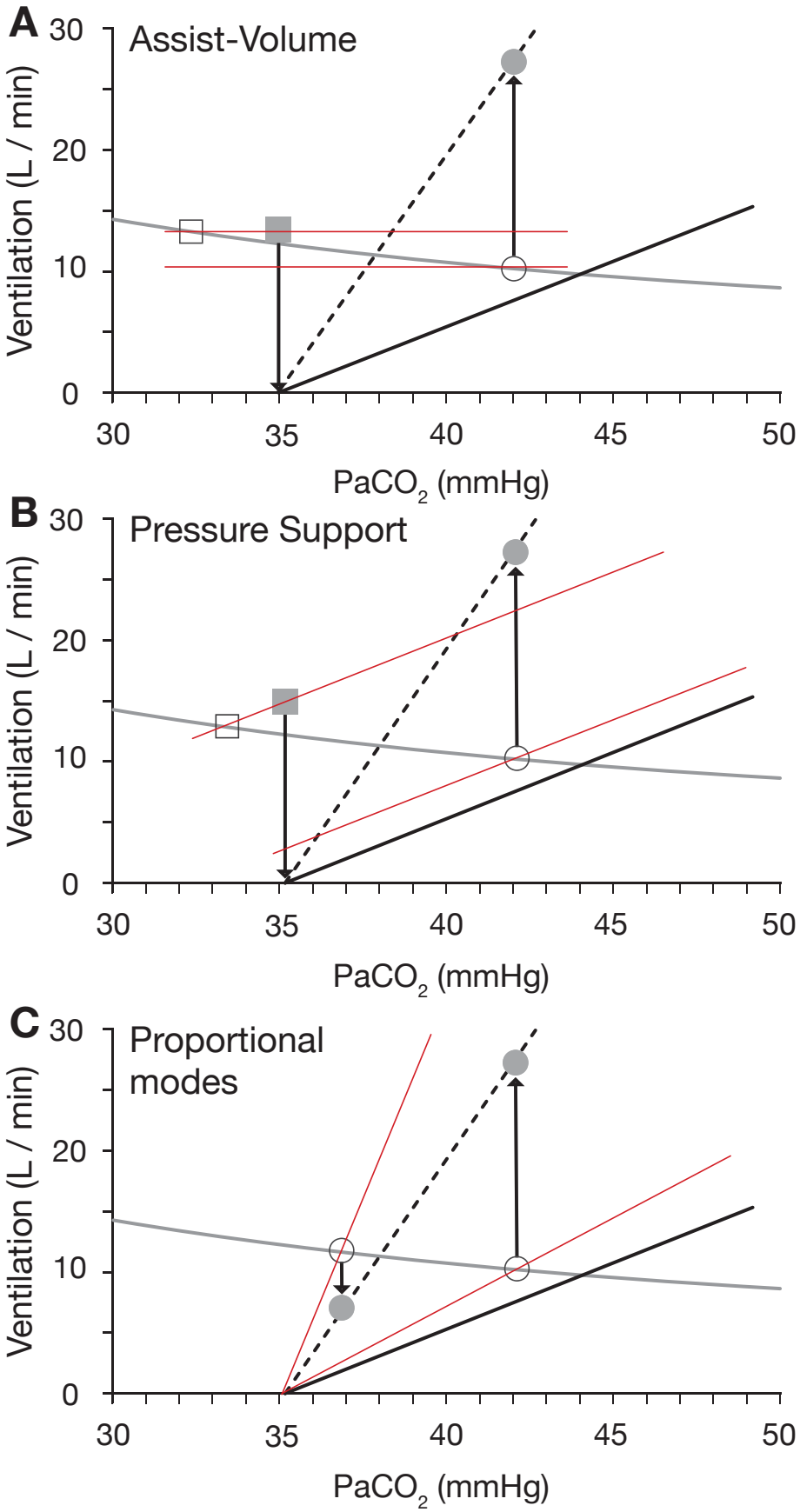

Figure 6

AJRCCM Articles in Press. Published on 22-August-2019 as 10.1164/rccm.201903-0596SO

On line data supplement

Respiratory Drive in Critically Ill Patients: Pathophysiology and Clinical Implications

Katerina Vaporidi[1], Evangelia Akoumianaki[1], Irene Telias[2,3], Ewan C. Goligher[2,4,5], Laurent Brochard[2,3*], Dimitris Georgopoulos[1*].

[1]Department of Intensive Care Medicine, University Hospital of Heraklion, Medical School University of Crete, Greece. [2]Interdepartmental Division of Critical Care Medicine, University of Toronto, Toronto, Canada. [3]Keenan Research Center and Li Ka Shing Knowledge Institute, St. Michael´s Hospital, Toronto, Canada. [4]Department of Medicine, University Health Network, Toronto, Canada. [5]Toronto General Hospital Research Institute, Toronto, Canada

*Equal contribution

Corresponding Author: D. Georgopoulos, Professor of Medicine,
Director of Intensive Care Medicine Department,
University Hospital of Heraklion, School of Medicine,
University of Crete, Heraklion, Crete, Greece
e-mail: georgopd@uoc.gr
Phone: +306944727501

AJRCCM Articles in Press. Published on 22-August-2019 as 10.1164/rccm.201903-0596SO

Effects of assisted mechanical ventilation on respiratory drive

To understand how mechanical ventilation affects the respiratory drive it is crucial to recognize the relationships between 1) peak inspiratory muscle pressure per breath ($Pmus_{peak}$) and tidal volume (V_T), and 2) $Pmus_{peak}$ and minute ventilation (V'_E) during un-assisted and assisted breathing. It is also essential to realize that because $Pmus_{peak}$ increases linearly with increasing $PaCO_2$ (1-4), these relationships are qualitatively similar to $PaCO_2$-V_T and $PaCO_2$-V'_E. During assisted breathing three modes of mechanical ventilation will be examined, a) assist volume control (AVC), b) pressure support (PS) and c) proportional assist (PAV+/NAVA). With AVC no back-up rate will be applied (back-up rate zero).

Figure E1: $Pmus_{peak}$– V_T relationship

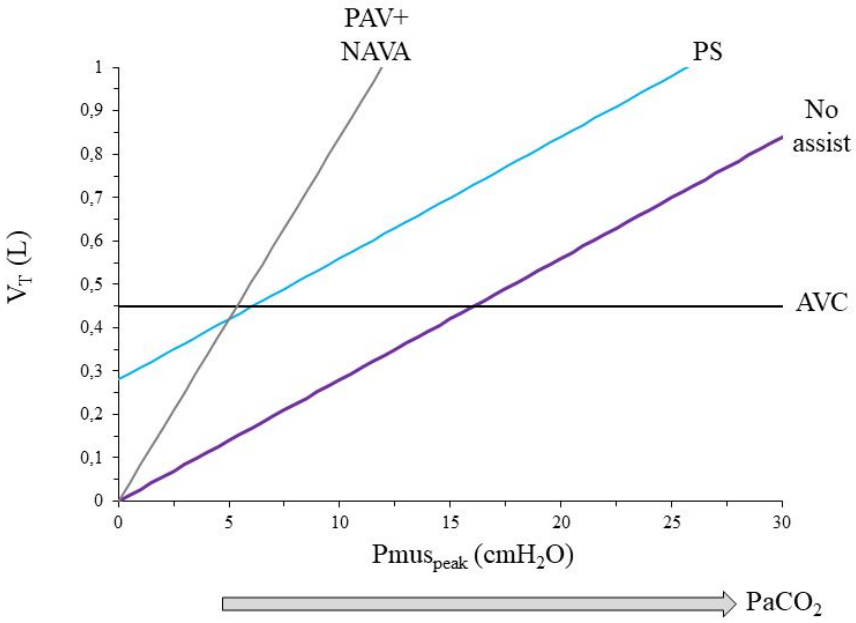

Relationship between $Pmus_{peak}$ (mainly determined by the respiratory drive) and V_T at constant respiratory system mechanics (elastance and resistance of respiratory system) and end-

expiratory lung volume in: a) unassisted spontaneous breathing (purple line), b) AVC (black line), c) PS (blue line) and d) PAV+/NAVA (gray line). During un-assisted breathing the slope of the relationship depends exclusively on respiratory system mechanics. With AVC the slope is always zero (horizontal line), while with PS there is a parallel up-ward shift of the un-assisted breathing line without affecting the slope. With both modes changing the level of assist does not affect the slope but changes the position of the corresponding curve (parallel up-ward or down-ward movements, not shown). Notice that with both modes even at very low $Pmus_{peak}$ (i.e. the patient relaxes all inspiratory muscles immediately after triggering due to low respiratory drive) V_T, depending on the level of assist, may be substantial. Compared to un-assisted breathing, proportional modes (PAV+/NAVA) increase the slope of $Pmus_{peak}$–V_T relationship depending on the level of assist. With PAV+/NAVA relaxation of inspiratory muscles immediately after triggering terminates the ventilator pressure and thus, even at very high assist (i.e. slope may approach 90^o degrees), V_T is zero or very close to zero. Because $Pmus_{peak}$ increases linearly with increasing $PaCO_2$ (gray thick arrow), $Pmus_{peak}$-V_T relationship is qualitatively similar to $PaCO_2$-V_T.

AJRCCM Articles in Press. Published on 22-August-2019 as 10.1164/rccm.201903-0596SO

Figure E2: $Pmus_{peak}$– V'_E relationship

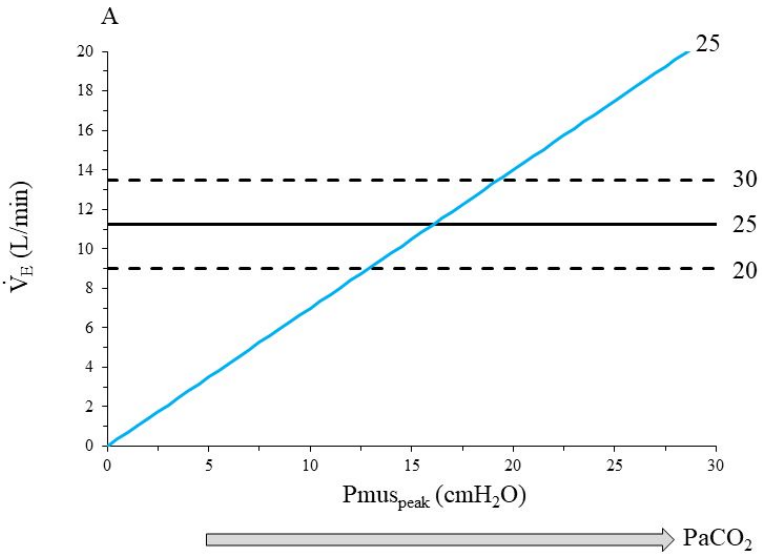

A: Relationship between $Pmus_{peak}$ and V'_E during unassisted and assisted breathing with AVC. Respiratory system mechanics and end-expiratory lung volume are considered constant. The number beside each curve indicates respiratory rate (breaths/min). The blue continuous line denotes the $Pmus_{peak}$-V'_E relationship during unassisted breathing. With AVC, V'_E at zero $Pmus_{peak}$ represents V'_E when the patient relaxes all inspiratory muscles immediately after triggering (minimum V'_E). With AVC at a respiratory rate similar to spontaneous breathing, the slope of the $Pmus_{peak}$-V'_E relationship is zero (black continuous line). Increases and decreases of respiratory rate at the same assist level, move the relationship upwards and downwards (black dashed lines), respectively, while the slope remains zero. Because $Pmus_{peak}$ increases linearly with increasing $PaCO_2$ (gray thick arrow), $Pmus_{peak}$-V'_E relationship is qualitatively similar to $PaCO_2$-V'_E.

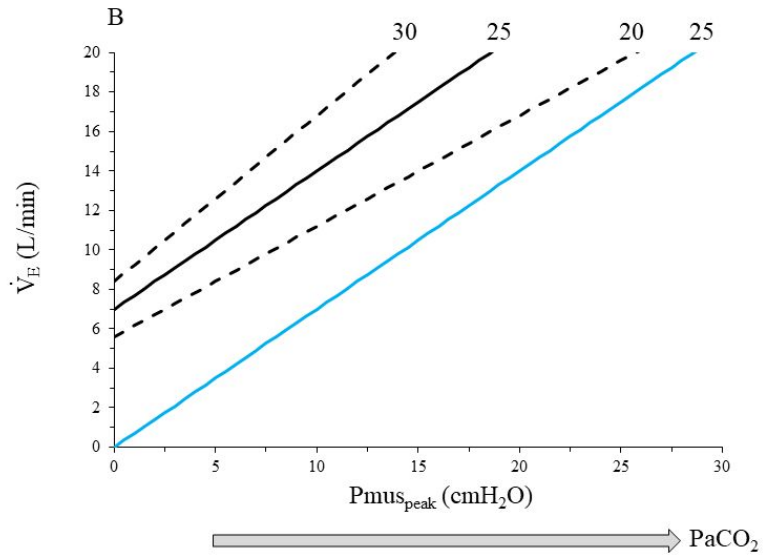

B: Relationship between $Pmus_{peak}$ and V'_E during unassisted and assisted breathing with PS. Respiratory system mechanics and end-expiratory lung volume are considered constant. The number beside each curve indicates respiratory rate (breaths/min). The blue continuous line denotes the $Pmus_{peak}$-V'_E relationship during unassisted breathing. With PS, V'_E at zero $Pmus_{peak}$ represents V'_E when the patient relaxes all inspiratory muscles immediately after triggering (minimum V'_E). At a respiratory rate similar to that during unassisted breathing, PS shifts the $Pmus_{peak}$-V'_E relationship parallel upwards (black continuous line) with a slope identical to the slope of the corresponding relationship during unassisted breathing. An increase of the respiratory rate at the same level of assist will move the relationship upwards (higher minimum V'_E) and increase its slope, while a decrease will move the relationship downwards (lower minimum V'_E) and decrease its slope (black dashed lines). Because $Pmus_{peak}$ increases linearly with increasing $PaCO_2$ (gray thick arrow), $Pmus_{peak}$-V'_E relationship is qualitatively similar to $PaCO_2$-V'_E.

AJRCCM Articles in Press. Published on 22-August-2019 as 10.1164/rccm.201903-0596SO

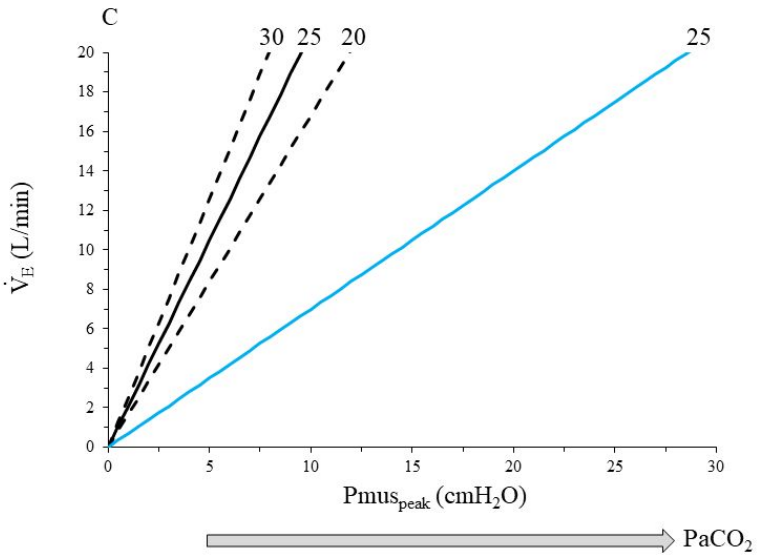

C: Relationship between $Pmus_{peak}$ and V'_E during unassisted and assisted breathing with PAV+/NAVA. Respiratory system mechanics and end-expiratory lung volume are considered constant. The number beside each curve indicates respiratory rate (breaths/min). The blue continuous line denotes the $Pmus_{peak}$-V'_E relationship during unassisted breathing. At a respiratory rate similar to that during unassisted breathing, PAV+/NAVA increase the slope of the $Pmus_{peak}$-V'_E relationship (black solid line). At the same assist level, this slope will be increased or decreased if respiratory rate increases or decreases, respectively (black dashed lines). Of note, with PAV+/NAVA minimum V'_E is always zero, irrespective of the level of assist (not shown) and respiratory rate. Because $Pmus_{peak}$ increases linearly with increasing $PaCO_2$ (gray thick arrow), $Pmus_{peak}$-V'_E relationship is qualitatively similar to $PaCO_2$-V'_E.

Mechanical ventilation and respiratory drive

In the following examples (Fig. E3-E6) a simplified analysis highlights the effects of assisted mechanical ventilation on respiratory drive in a patient with impaired respiratory system mechanics. The brain and ventilation curves, and the relationships between $PaCO_2$ and V'_E are presented for the three main modes of assisted mechanical ventilation, AVC, PS and PAV+/NAVA. In each mode four levels of assist are applied. A dead space per breath (V_D) to V_T ratio (V_D/V_T) of 0.5 and CO_2 production ($V'CO_2$) of 250 ml/min are used to construct the metabolic hyperbola (gray continuous line) as follows:

$$PaCO_2=0.863*V'CO_2/[V'_E*(1-V_D/V_T)], \text{ Eq. 1.}$$

For simplicity, the metabolic hyperbola is considered constant with and without mechanical ventilation. In reality mechanical ventilation may change both $V'CO_2$ (by altering the work of breathing) and V_D/V_T, and thus shift the metabolic hyperbola downward or upward.

The slope of the brain curve (black dashed line), representing the sensitivity to CO_2 or the ventilatory demands at a given $PaCO_2$, is set at 5.75 l/min/mmHg. A relatively high slope is used (normal range 2-8 l/min/mmHg), to account for conditions commonly present in critically ill patients such as metabolic acidosis, stimulation of lung and chest wall receptors, or sepsis. The slope of the un-assisted ventilation curve (black continuous line) is set at 0.95 l/min/mmHg, to account for the derangement in respiratory system mechanics (i.e. high respiratory system elastance, Ers). The patient is considered to be sedated and an apneic threshold is set at $PaCO_2$ of 36 mmHg. The same brain and un-assisted ventilation curves are used in all examples. Also, for simplicity it is assumed that a) all patient efforts trigger the ventilator (no ineffective efforts), b) end-expiratory lung volume is constant and c) respiratory rate remains the same between un-assisted and assisted breathing. The later assumption is valid, since respiratory rate may change minimally with mechanical ventilation and the level of assist, particularly at low and moderate levels of respiratory drive. See also Figure E2 (A-C) for the effect of a change in respiratory rate on the ventilation curve.

AJRCCM Articles in Press. Published on 22-August-2019 as 10.1164/rccm.201903-0596SO

In this example respiratory rate of 25 breaths/min is applied and assuming a ratio of inspiratory to total breath duration (T_I/T_{TOT}) of 0.3, inspiratory time of 0.72 sec is derived. At a given $PaCO_2$ the respiratory drive is quantified as the tidal volume V_{Tbrain} desired by the respiratory center to inspiratory time (T_I). V_{Tbrain} is calculated by dividing the ventilatory demands, as dictated by the brain curve at the given $PaCO_2$ (V'_{Ebrain}), with the respiratory rate (25 br/min), used in the example: $V_{Tbrain} = V'_{Ebrain} / 25$.

Figure E3: Un-assisted breathing

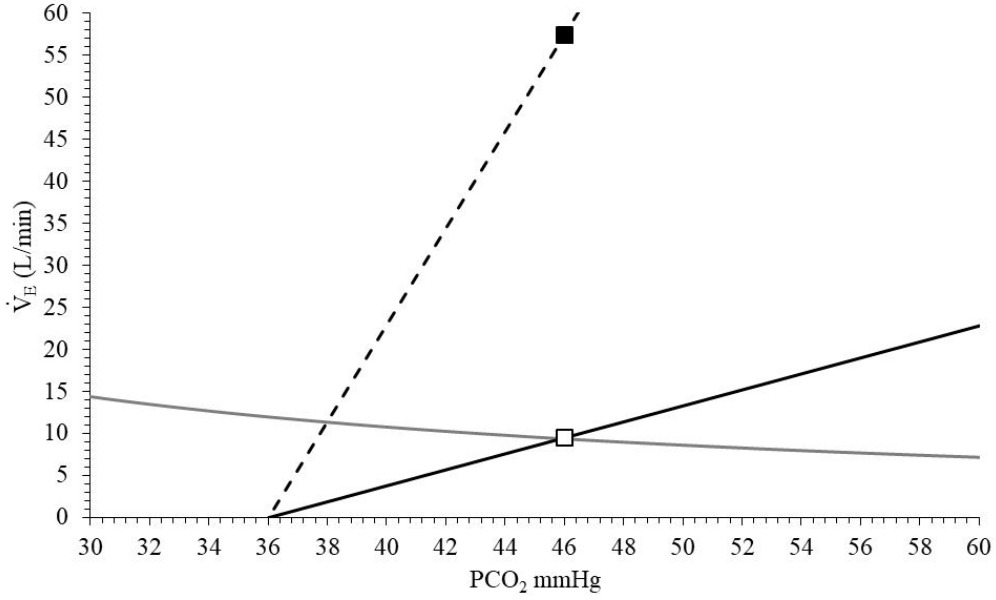

Relationships between $PaCO_2$ and V'_E during un-assisted breathing. The $PaCO_2$ desired by the brain is 38 mmHg (intersection between metabolic hyperbola and brain curve), while the actual $PaCO_2$ is 46 mmHg (intersection between un-assisted ventilation curve and metabolic hyperbola, open square). At a $PaCO_2$ of 46 mmHg the respiratory center demands 57.5 l/min of ventilation (V'_{Ebrain}, black square) as dictated by the brain curve, while actual V'_E is 9.4 l/min (open square). At this V'_{Ebrain} the desired V_T (V_{Tbrain}) is 2.3 l (57.5/25) and respiratory drive (V_{Tbrain}/T_I) is 3.2 l/sec (2.3/0.72). During un-assisted breathing this respiratory drive is similar to that obtained at moderate exercise. The ventilatory demands (V'_{Ebrain}=57.5

l/min) are not met (actual V'_E=9.4 l/min). The magnitude of unmet demands depends on $PaCO_2$ and the slopes of brain and ventilator curves.

Figure E4 – Assist Volume Control (no back-up rate)

Relationships between $PaCO_2$ and minute ventilation during different levels of AVC (A-D, from low to high assist). With AVC V_T is preset so un-assisted ventilation curve is shifted up-ward and its slope becomes zero (horizontal to $PaCO_2$ axis) over a wide range of $PaCO_2$ (blue continuous line). Notice that at high $PaCO_2$ ventilation may increase due to progressive increase of patient respiratory rate, a common response pattern when V_T is constrained (blue dashed line).

For clarity of presentation the scale is increased in Figures 3B, 3C and 3D.

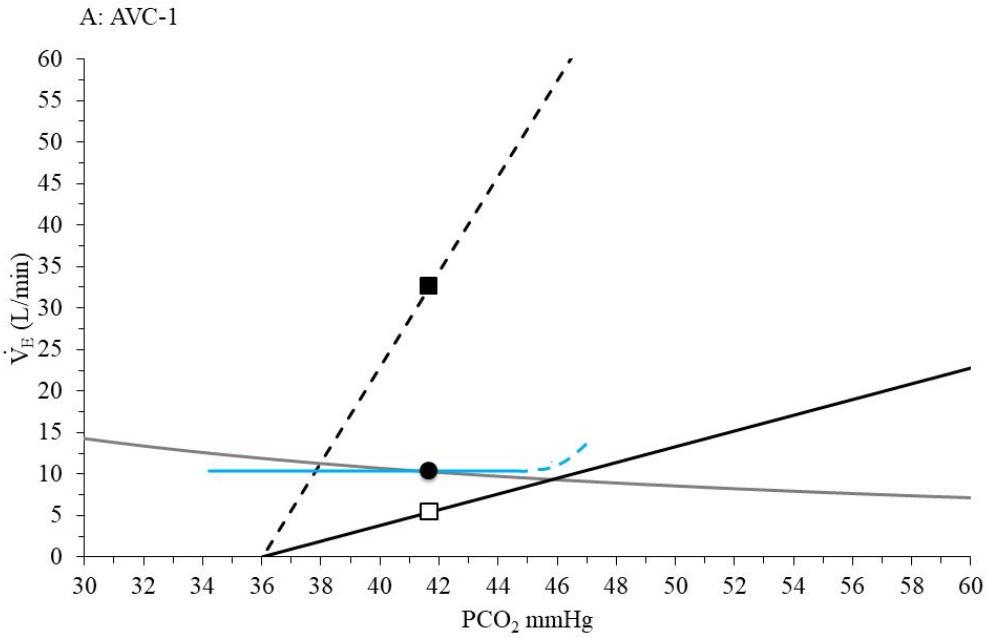

A: With AVC-1 $PaCO_2$ (black circle, intersection between the new ventilation curve and metabolic hyperbola) is 41.7 mmHg. Now, at a $PaCO_2$ of 41.7 mmHg the respiratory center (brain curve) demands 32.8 l/min of ventilation (V'_{Ebrain}, black square) which corresponds to V_{Tbrain} of 1.31 l (32.8/25) and respiratory drive (V_{Tbrain}/T_I) of 1.82 l/sec. Yet, the actual V'_E is

AJRCCM Articles in Press. Published on 22-August-2019 as 10.1164/rccm.201903-0596SO

10.4 l/min (black circle). To achieve 10.4 l/min the patient contributes 5.4 l/min (open square, un-assisted ventilation curve) and the ventilator 5 l/min. The unmet demands are 22.4 l/min, due to dissociation between brain (black dashed line) and ventilation curve with AVC-1 (blue continuous line). Compared to un-assisted breathing AVC-1 decreases respiratory drive by 43% (from 3.2 l/sec to 1.82 l/sec).

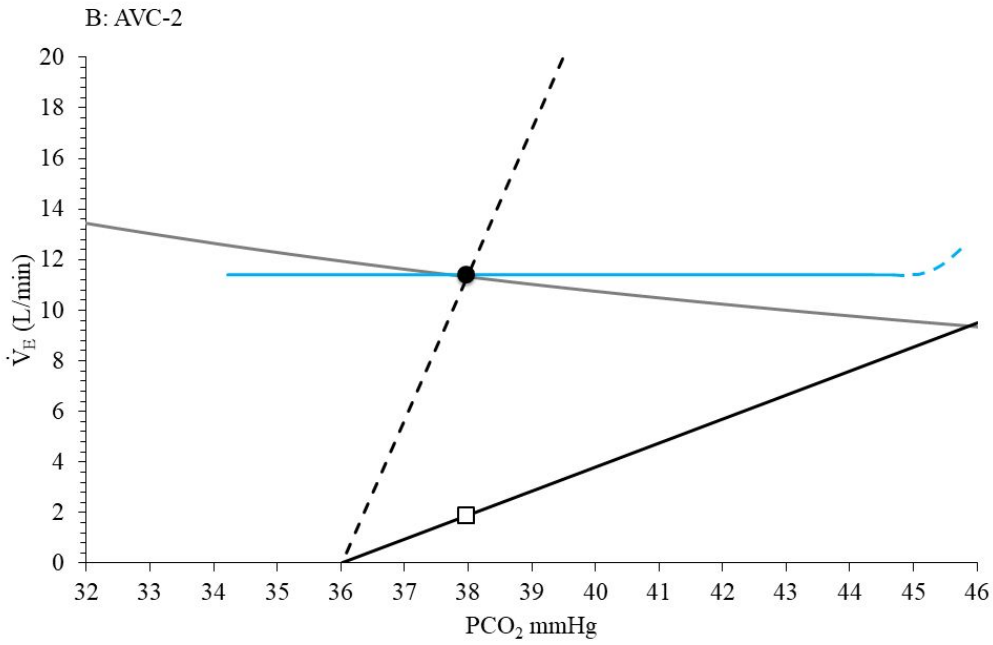

B: With AVC-2 $PaCO_2$ (black circle, intersection point between the new ventilation curve and metabolic hyperbola) is 38 mmHg. Now, by chance, the intersection between the new ventilation curve and metabolic hyperbola is similar to that between brain curve and metabolic hyperbola. At $PaCO_2$ of 38 mmHg the respiratory center demands 11.4 l/min of ventilation. Since the actual $PaCO_2$ is similar to that desired by the respiratory center, the ventilatory demands are met by the delivered ventilation and V_{Tbrain} equals the actual V_T (0.46 l). The respiratory drive is 0.63 l/sec and is satisfied by actual V_T/T_I (mean inspiratory flow). To achieve 11.4 l/min the patient contributes 1.9 l/min (open square, un-assisted ventilation curve) and the ventilator 9.5 l/min. Compared to un-assisted breathing AVC-2 decreases respiratory drive by 80% (from 3.2 l/sec to 0.63 l/sec).

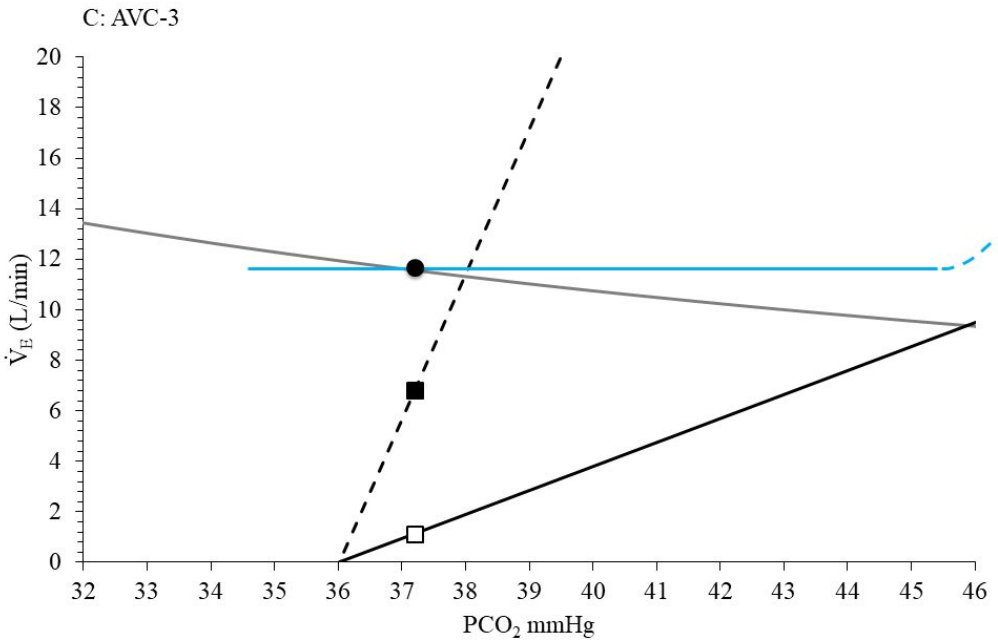

C: With AVC-3 $PaCO_2$ (black circle, intersection point between the new ventilation curve and metabolic hyperbola) is 37.2 mmHg, lower than that desired by the brain. At $PaCO_2$ of 37.2 mmHg the respiratory center demands 6.9 l/min of ventilation (black square), V_{Tbrain} is 0.28 l and the respiratory drive (V_{Tbrain}/T_I) is 0.38 l/sec. Actual ventilation is 11.6 l/min. To achieve 11.6 l/min the patient contributes 1.1 l/min (open square, un-assisted ventilation curve) and the ventilator 10.5 l/min. Compared to un-assisted breathing AVC-3 decreases respiratory drive by 88% (from 3.2 l/sec to 0.38 l/sec).

AJRCCM Articles in Press. Published on 22-August-2019 as 10.1164/rccm.201903-0596SO

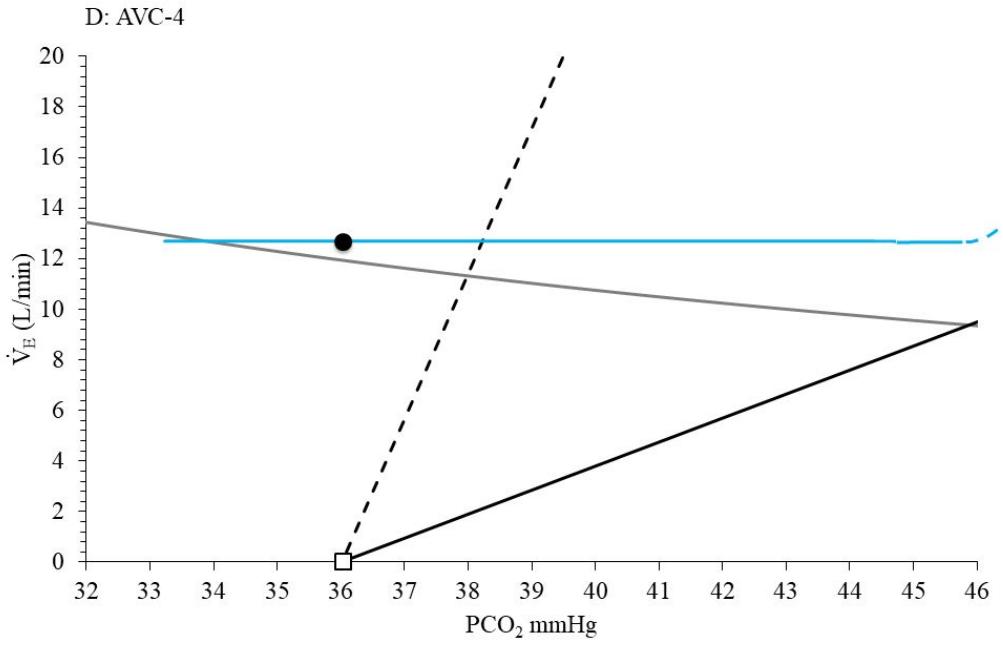

D: Although with AVC-4 the new ventilation curve (blue continuous line) intersects the metabolic hyperbola at $PaCO_2$ of 34 mmHg, the actual PaCO2 is around 36 mmHg (black circle). Steady-state cannot be achieved because the occurrence of apneas prevents the $PaCO_2$ to drop below 36 mmHg (apneic threshold). At $PaCO_2$ of 36 mmHg respiratory center's output is zero (open square) and the patient exhibits periodic breathing. Respiratory drive hovers around zero (no steady-state). When the patient relaxes the diaphragm immediately after triggering (i.e. when between apneas respiratory drive is slightly above zero), the ventilator provides passively approximately 13.5 l/min (black circle). Ventilation ranges between zero (apnea) and approximately 13.5 l/min. Because inspiration is passive the patient is at risk of diaphragmatic atrophy.

Figure E5 – Pressure Support

Relationships between $PaCO_2$ and minute ventilation during different levels of PS (A-D, from low to high PS). At constant respiratory rate, PS causes a parallel up-ward deviation of the un-assisted ventilation curve. The magnitude of the deviation depends on PS level, mechanics of respiratory system, rising time and cycling off criterion.

For clarity of presentation the scale is increased in Figures E5B, E5C and E5D.

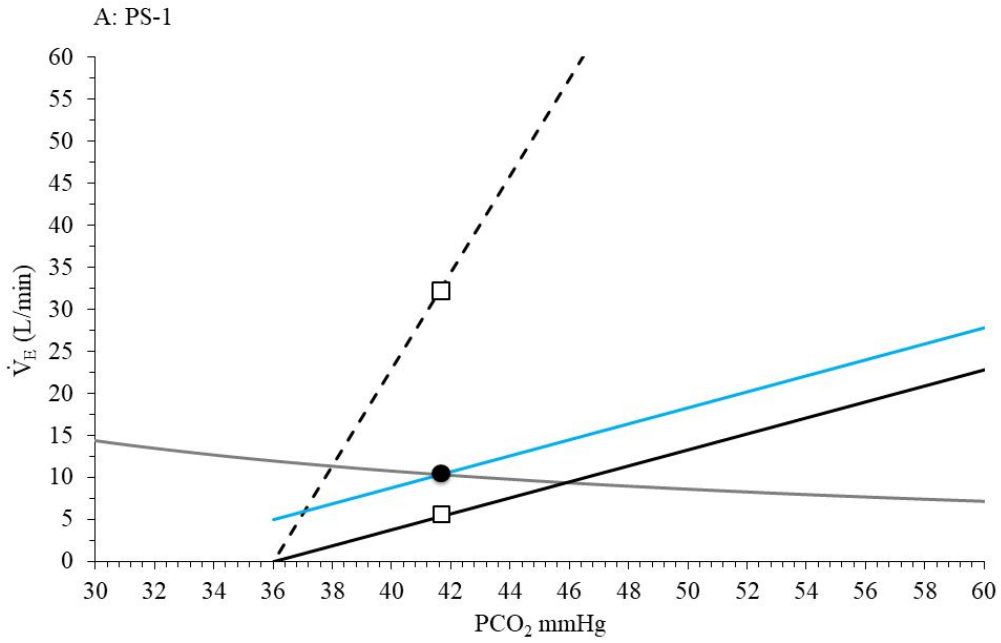

A: With PS-1 $PaCO_2$ (black circle, intersection between the new ventilation curve and metabolic hyperbola) is 41.7 mmHg. Now, at a $PaCO_2$ of 41.7 mmHg the respiratory center (brain curve) demands 32.8 l/min of ventilation (V'_{Ebrain}, black square) which corresponds to V_{Tbrain} of 1.31 l (32.8/25) and respiratory drive (V_{Tbrain}/T_I) of 1.82 l/sec. Yet, the actual V'_E is 10.4 l/min (black circle). To achieve 10.4 l/min the patient contributes 5.4 l/min (open square, un-assisted ventilation curve) and the ventilator 5 l/min. The unmet demands are 22.4 l/min, due to dissociation between brain (black dashed line) and ventilation curve with PS-1 (blue continuous line). Compared to un-assisted breathing PS-1 decreases respiratory drive by 43% (from 3.2 l/sec to 1.82 l/sec).

AJRCCM Articles in Press. Published on 22-August-2019 as 10.1164/rccm.201903-0596SO

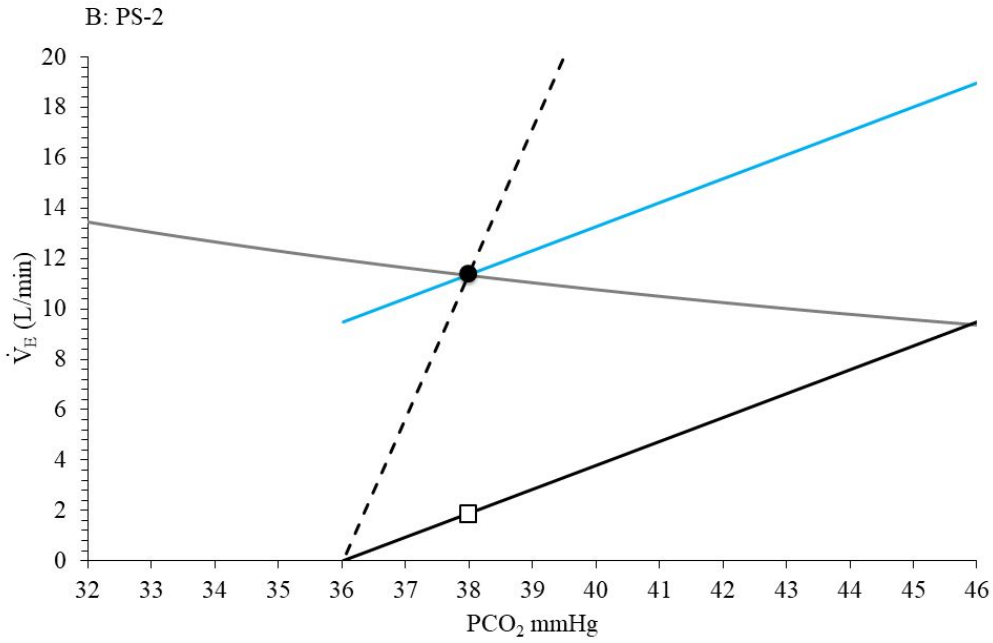

B: With PS-2 $PaCO_2$ (black circle, intersection point between the new ventilation curve and metabolic hyperbola) is 38 mmHg. Now, by chance, the intersection between the new ventilation curve and metabolic hyperbola is similar to that between brain curve and metabolic hyperbola. At $PaCO_2$ of 38 mmHg the respiratory center demands 11.4 l/min of ventilation. Since the actual $PaCO_2$ is similar to that desired by the respiratory center, the ventilatory demands are met by the delivered ventilation and V_{Tbrain} equals the actual V_T (0.46 l). The respiratory drive is 0.63 l/sec and is satisfied by actual V_T/T_I (mean inspiratory flow). To achieve 11.4 l/min the patient contributes 1.9 l/min (open square, un-assisted ventilation curve) and the ventilator 9.5 l/min. Compared to un-assisted breathing PS-2 decreases respiratory drive by 80% (from 3.2 l/sec to 0.63 l/sec).

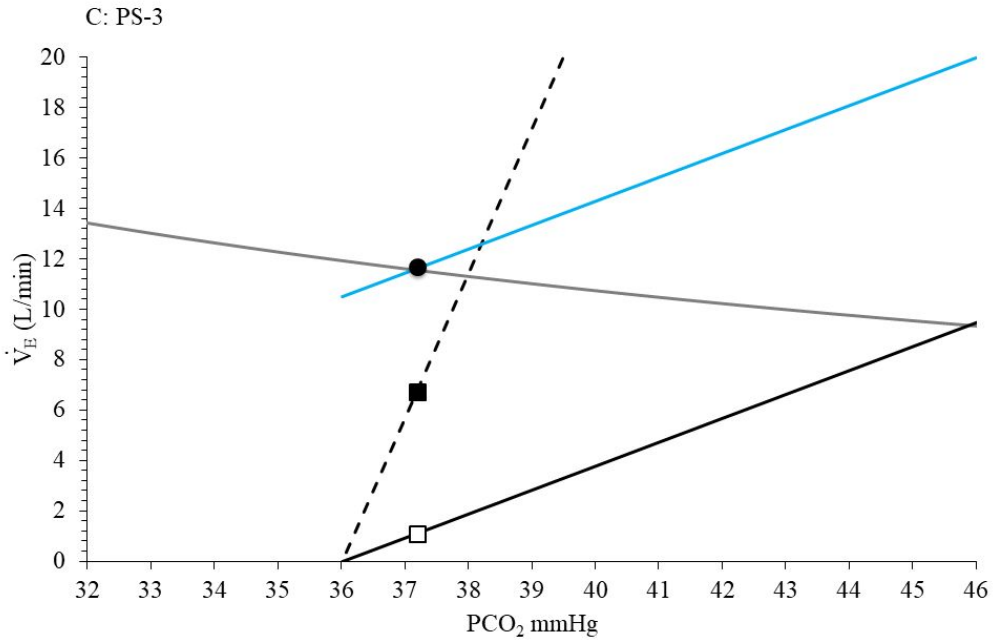

C: With PS-3 $PaCO_2$ (black circle, intersection point between the new ventilation curve and metabolic hyperbola) is 37.2 mmHg, lower than that desired by the brain. At $PaCO_2$ of 37.2 mmHg the respiratory center demands 6.9 l/min of ventilation (black square), V_{Tbrain} is 0.28 l and the respiratory drive (V_{Tbrain}/T_I) is 0.38 l/sec. Actual ventilation is 11.6 l/min. To achieve 11.6 l/min the patient contributes 1.1 l/min (open square, un-assisted ventilation curve) and the ventilator 10.5 l/min. Compared to un-assisted breathing PS-3 decreases respiratory drive by 88% (from 3.2 l/sec to 0.38 l/sec).

AJRCCM Articles in Press. Published on 22-August-2019 as 10.1164/rccm.201903-0596SO

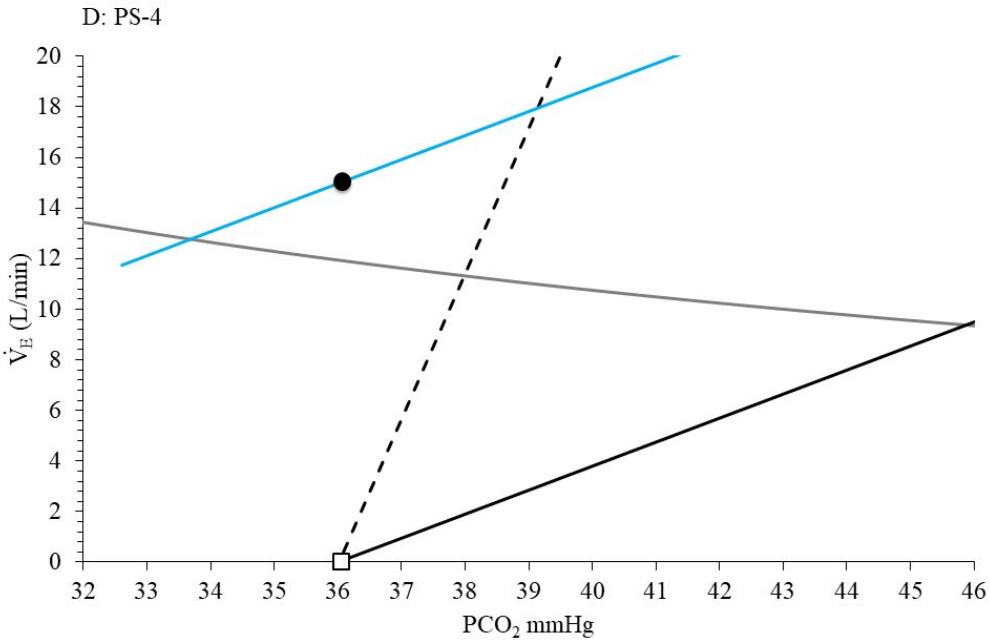

D: Although with PS-4 the new ventilation curve (blue line) intersects the metabolic hyperbola at $PaCO_2$ of 33.8 mmHg, the actual PaCO2 is around 36 mmHg (black circle). Steady-state cannot be achieved because the occurrence of apneas prevents the $PaCO_2$ to drop below 36 mmHg (apneic threshold). At $PaCO_2$ of 36 mmHg respiratory center's output is zero (open square) and the patient exhibits periodic breathing. Respiratory drive hovers around zero (no steady-state). When the patient relaxes the diaphragm immediately after triggering (i.e. when, between apneas, the respiratory drive is slightly above zero), the ventilator provides passively approximately 14.5 l/min (black circle). Ventilation ranges between zero (apnea) and approximately 14.5 l/min. Because inspiration is passive the patient is at risk of diaphragmatic atrophy. Compared to AVC-4, with PS-4 apneas will last longer due to higher ventilation when the patient triggers the ventilator.

Figure E6 – Proportional modes

Relationships between $PaCO_2$ and minute ventilation during different levels of PAV+/NAVA (A-D, from low to high assist). At constant respiratory rate, PAV+/NAVA increases the slope of un-assisted ventilation curve. The starting point of the ventilation curve with PAV+/NAVA is similar to that of un-assisted ventilation curve ($PaCO_2$ 36 mmHg, apneic threshold). The slope of the assisted ventilation curve depends on respiratory system mechanics and level of assist.

For clarity of presentation the scale is increased in Figures E6B, E6C and E6D.

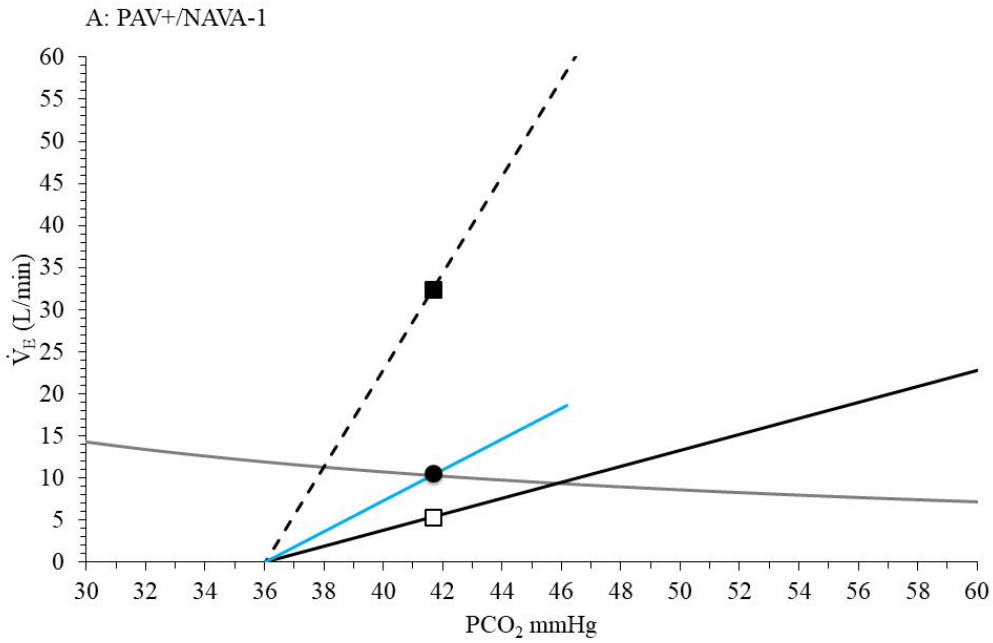

A: With PAV+/NAVA-1 $PaCO_2$ (black circle, intersection between the new ventilation curve and metabolic hyperbola) is 41.7 mmHg. Now, at a $PaCO_2$ of 41.7 mmHg the respiratory center (brain curve) demands 32.8 l/min of ventilation (V'_{Ebrain}, black square) which corresponds to V_{Tbrain} of 1.31 l (32.8/25) and respiratory drive (V_{Tbrain}/T_I) of 1.82 l/sec. Yet, the actual V'_E is 10.4 l/min (black circle). To achieve 10.4 l/min the patient contributes 5.4 l/min (open square, un-assisted ventilation curve) and the ventilator 5 l/min. The unmet demands are 22.4 l/min, due to dissociation between brain (black dashed line) and ventilation curve

AJRCCM Articles in Press. Published on 22-August-2019 as 10.1164/rccm.201903-0596SO

with PAV+/NAVA-1 (blue continuous line). Compared to un-assisted breathing PAV+/NAVA-1 decreases respiratory drive by 43% (from 3.2 l/sec to 1.82 l/sec).

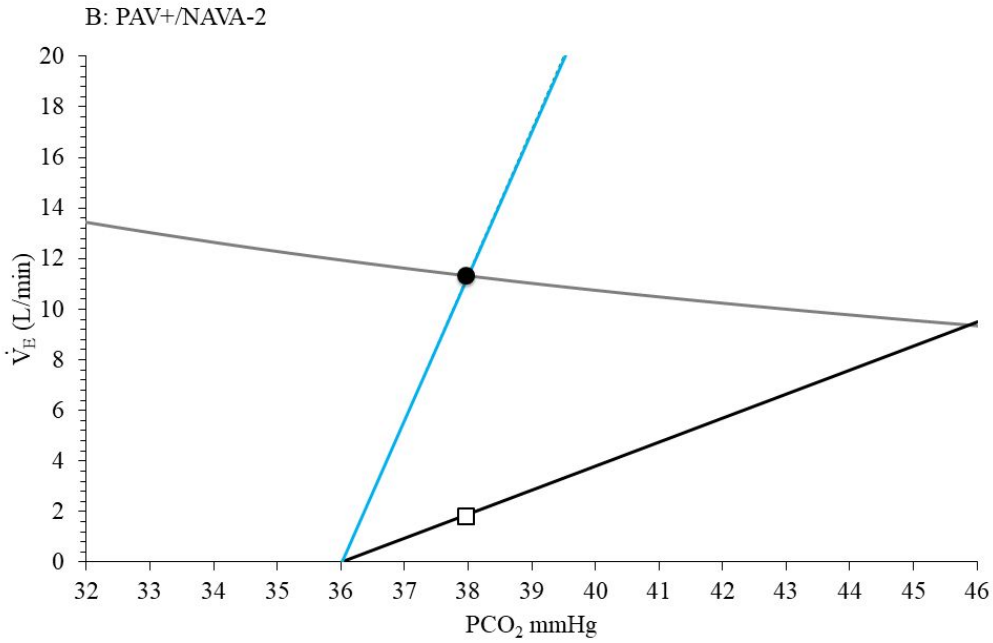

B: With PAV+/NAVA-2 $PaCO_2$ (black circle, intersection point between the new ventilation curve and metabolic hyperbola) is 38 mmHg. Now, by chance, the intersection between the new ventilation curve and metabolic hyperbola is similar to that between brain curve and metabolic hyperbola. At $PaCO_2$ of 38 mmHg the respiratory center demands 11.4 l/min of ventilation. Since the actual $PaCO_2$ is similar to that desired by the respiratory center, the ventilatory demands are met by the delivered ventilation and V_{Tbrain} equals the actual V_T (0.46 l). The respiratory drive is 0.63 l/sec and is satisfied by actual V_T/T_I (mean inspiratory flow). To achieve 11.4 l/min the patient contributes 1.9 l/min (open square, un-assisted ventilation curve) and the ventilator 9.5 l/min. Compared to un-assisted breathing PAV+/NAVA-2 decreases respiratory drive by 80% (from 3.2 l/sec to 0.63 l/sec).

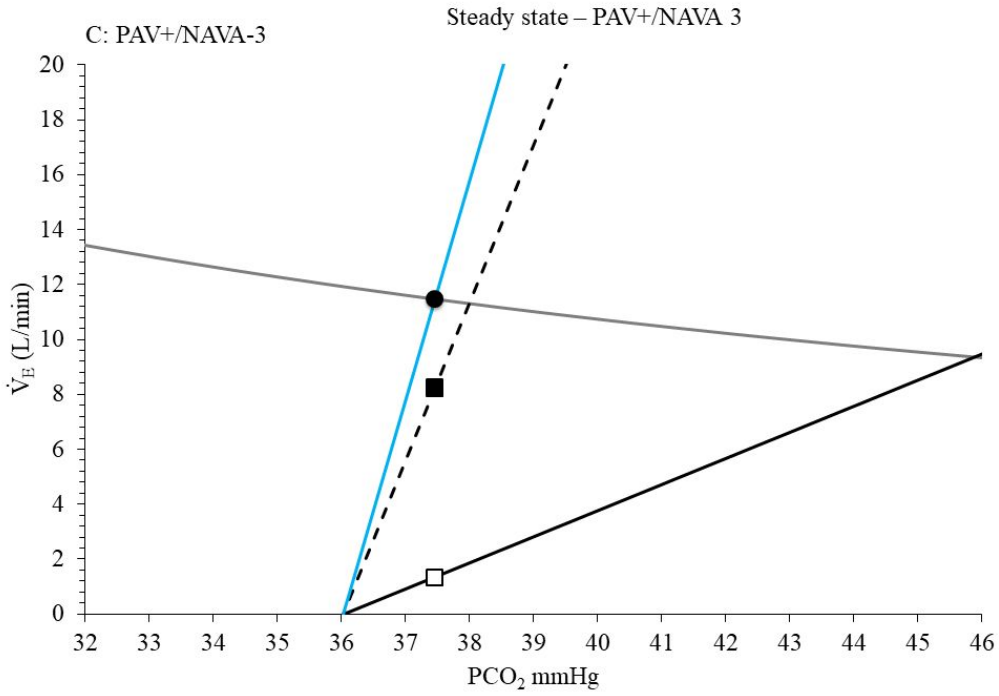

C: With PAV+/NAVA-3 $PaCO_2$ (black circle, intersection point between the new ventilation curve and metabolic hyperbola) is 37.4 mmHg, lower than that desired by the brain. At $PaCO_2$ of 37.2 mmHg the respiratory center demands 8.0 l/min of ventilation (black square), V_{Tbrain} is 0.32 l and the respiratory drive (V_{Tbrain}/T_I) is 0.44 l/sec. Actual ventilation is 11.5 l/min. To achieve 11.5 l/min the patient contributes 1.0 l/min (open square, un-assisted ventilation curve) and the ventilator 10.5 l/min. Compared to un-assisted breathing PAV+/NAVA-3 decreases respiratory drive by 86% (from 3.2 l/sec to 0.44 l/sec).

AJRCCM Articles in Press. Published on 22-August-2019 as 10.1164/rccm.201903-0596SO

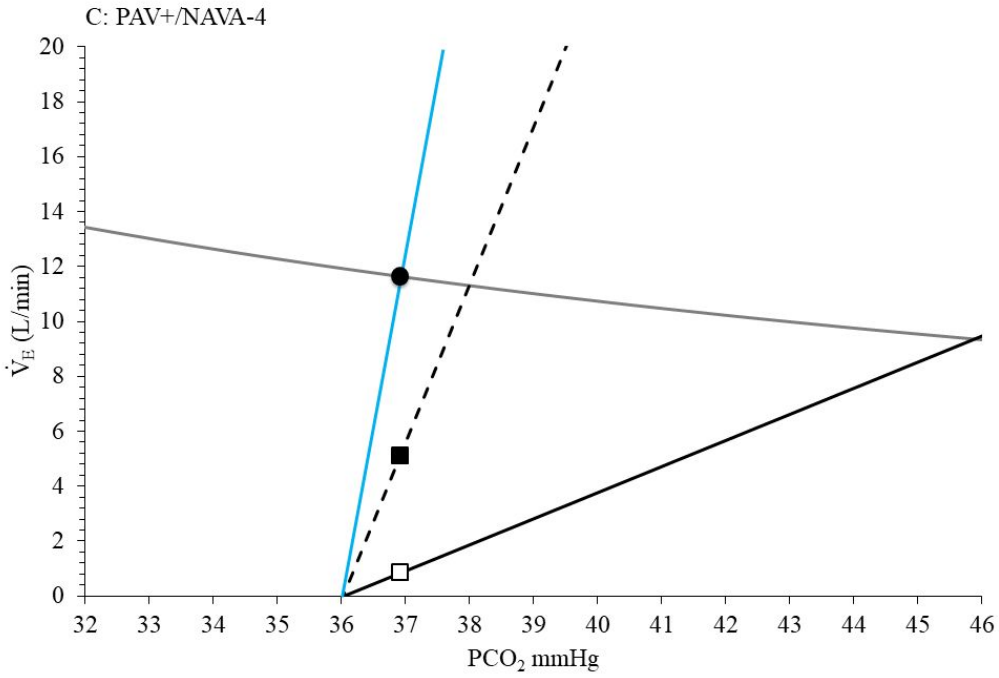

D: With PAV+/NAVA-4 (highest possible assist at least with PAV+, amplification factor close to 10) $PaCO_2$ (black circle, intersection point between the new ventilation curve and metabolic hyperbola) is 36.9 mmHg, lower than that desired by the brain. At $PaCO_2$ of 36.9 mmHg the respiratory center demands 5.2 l/min of ventilation (black square), V_{Tbrain} is 0.21 l and the respiratory drive (V_{Tbrain}/T_I) is 0.29 l/sec. Actual ventilation is 11.7 l/min. To achieve 11.7 l/min the patient contributes 0.86 l/min (open square, un-assisted ventilation curve) and the ventilator 10.8 l/min. Compared to un-assisted breathing PAV+/NAVA-4 decreases respiratory drive by 91% (from 3.2 l/sec to 0.29 l/sec). Contrary to PS and AVC, even at very high assist (slope of ventilation curve slightly lower than 90°) steady state is achieved.

References

1. Clark FJ, von Euler C. On the regulation of depth and rate of breathing. *The Journal of physiology* 1972; 222: 267-295.

2. Duffin J, Mohan RM, Vasiliou P, Stephenson R, Mahamed S. A model of the chemoreflex control of breathing in humans: model parameters measurement. *Respiration physiology* 2000; 120: 13-26.

3. Georgopoulos D, Mitrouska I, Bshouty Z, Webster K, Patakas D, Younes M. Respiratory response to CO2 during pressure-support ventilation in conscious normal humans. *American journal of respiratory and critical care medicine* 1997; 156: 146-154.

4. Georgopoulos D, Mitrouska I, Webster K, Bshouty Z, Younes M. Effects of inspiratory muscle unloading on the response of respiratory motor output to CO2. *American journal of respiratory and critical care medicine* 1997; 155: 2000-2009.